

1 **Title:** Efficient genome-wide sequencing and low coverage pedigree analysis from non-  
2 invasively collected samples

3

4 **Authors**

5 Noah Snyder-Mackler<sup>1</sup>, William H. Majoros<sup>2</sup>, Michael L. Yuan<sup>1</sup>, Amanda O. Shaver<sup>1</sup>,  
6 Jacob B. Gordon<sup>3</sup>, Gisela H. Kopp<sup>4</sup>, Stephen A. Schlebusch<sup>5</sup>, Jeffrey D. Wall<sup>6</sup>, Susan C.  
7 Alberts<sup>3,7</sup>, Sayan Mukherjee<sup>8,9,10</sup>, Xiang Zhou<sup>\*,11,12</sup>, Jenny Tung<sup>\*,13,7,13</sup>

8 **Author Affiliations**

9 <sup>1</sup> Department of Evolutionary Anthropology, Duke University, Durham, NC

10 <sup>2</sup> Graduate Program in Computational Biology and Bioinformatics, Duke University,  
11 Durham, NC

12 <sup>3</sup> Department of Biology, Duke University, Durham, NC

13 <sup>4</sup> Cognitive Ethology Laboratory, German Primate Center, Leibniz Institute for Primate  
14 Research, Göttingen, Germany

15 <sup>5</sup> Department of Molecular and Cell Biology, University of Cape Town, Cape Town,  
16 South Africa

17 <sup>6</sup> Institute for Human Genetics, University of California San Francisco, San Francisco,  
18 CA

19 <sup>7</sup> Institute of Primate Research, National Museums of Kenya, Nairobi, Kenya

20 <sup>8</sup> Department of Statistical Science, Duke University, Durham, NC

21 <sup>9</sup> Department of Mathematics, Duke University, Durham, NC

22 <sup>10</sup> Department of Computer Science, Duke University, Durham, NC

23 <sup>11</sup> Department of Biostatistics, University of Michigan, Ann Arbor, MI

24 <sup>12</sup> Center for Statistical Genetics, University of Michigan, Ann Arbor, MI

25 <sup>13</sup> Duke University Population Research Institute, Duke University, Durham, NC 27708

26

27 **Keywords:** Capture-based enrichment, non-invasive samples, baboons, paternity

28 analysis, pedigree, genome resequencing

29

30 **\*Authors for Correspondence**

31 Jenny Tung

32 Department of Evolutionary Anthropology, Duke University

33 104 Biological Sciences Building, Box 90383

34 Durham, NC 27708-9976

35 Fax: 919-660-7348; Phone: 919-684-3910

36 E-mail: [jt5@duke.edu](mailto:jt5@duke.edu)

37

38 Xiang Zhou

39 Department of Biostatistics, University of Michigan

40 1415 Washington Heights #4623

41 Ann Arbor, MI 48109

42 Phone: 734-764-7067

43 E-mail: [xzhousph@umich.edu](mailto:xzhousph@umich.edu)

44

45 **Running title:** Genomic enrichment of non-invasive samples

46

47 **ABSTRACT:**

48           Research on the genetics of natural populations was revolutionized in the 1990's  
49 by methods for genotyping non-invasively collected samples. However, these methods  
50 have remained largely unchanged for the past 20 years and lag far behind the genomics  
51 era. To close this gap, here we report an optimized laboratory protocol for genome-wide  
52 capture of endogenous DNA from non-invasively collected samples, coupled with a  
53 novel computational approach to reconstruct pedigree links from the resulting low-  
54 coverage data. We validated both methods using fecal samples from 62 wild baboons,  
55 including 48 from an independently constructed extended pedigree. We enriched fecal-  
56 derived DNA samples up to 40-fold for endogenous baboon DNA, and reconstructed  
57 near-perfect pedigree relationships even with extremely low-coverage sequencing. We  
58 anticipate that these methods will be broadly applicable to the many research systems  
59 for which only non-invasive samples are available. The lab protocol and software  
60 ("*WHODAD*") are freely available at [www.tung-lab.org/protocols](http://www.tung-lab.org/protocols) and  
61 [www.xzlab.org/software](http://www.xzlab.org/software), respectively.

62

63

64           The capacity to generate genetic data from low-quality or non-invasively  
65 collected samples, first developed in the 1990's<sup>1,2</sup>, revolutionized the study of genetics,  
66 evolution, behavior, and ecology in natural populations. These methodological  
67 advances facilitated phylogenetic and phylogeographic analyses of difficult-to-sample  
68 taxa<sup>3-5</sup>; helped define the role of admixture in mammalian evolution<sup>6-8</sup>; and enabled  
69 theoretical expectations about paternal investment, kin recognition, and reproductive  
70 skew to be empirically tested, sometimes for the first time<sup>9-12</sup>. They also yielded  
71 important insights into the genetic viability and future prospects of threatened or  
72 endangered populations from which invasive samples are impossible to obtain<sup>13-17</sup>.  
73 Non-invasive genetic analysis has thus changed the ways we study population,  
74 ecological, and conservation genetics. Indeed, these fields would look very different  
75 today—and we would know far less about many species—without it.

76           However, techniques for non-invasive genetic analysis have changed little in the  
77 past twenty years. Collection of genetic data from non-invasively collected tissues (e.g.,  
78 feces, hair, urine) continues to be labor-intensive, time-intensive, and vulnerable to  
79 technical artifacts such as allelic dropout and cross-contamination<sup>18,19</sup>. Further, current  
80 methods ultimately yield very small amounts of data by today's standards. Typical  
81 studies genotype only a dozen to several dozen microsatellite loci per individual – a  
82 trivial amount compared to the data sets now routinely generated using standard high-  
83 throughput sequencing approaches. Thus, while existing methods are sufficient for  
84 basic pedigree construction and estimating some population genetic parameters  
85 (although usually with substantial uncertainty), they are severely underpowered for  
86 many other types of analyses, such as identifying signatures of natural selection,

87 reconstructing population history and demography, and testing for genetic associations  
88 with phenotypic variation<sup>20-22</sup>. Similarly, analyses that require local (i.e., gene- or region-  
89 specific) information on genetic diversity, structure, or ancestry instead of genome-wide  
90 averages cannot be conducted<sup>23-27</sup>. Finally, because non-invasively collected genotype  
91 data are most often based on microsatellites, they cannot take advantage of new tools  
92 designed specifically for single nucleotide variants<sup>28-30</sup>.

93         Generating genome-scale data sets from non-invasive samples is challenging for  
94 two reasons. First, in many cases, the DNA extracted from these samples is low quality  
95 and highly fragmented. Second, it contains large proportions of non-host DNA. For  
96 example, only about 1% of DNA extracted from fecal-derived samples is endogenous to  
97 the donor animal (most is microbial)<sup>31</sup>. Sequence capture methods, in which  
98 synthesized baits are used to enrich for pre-specified target sequences from a larger  
99 DNA pool<sup>32</sup>, present a potential solution to both of these problems. Because shearing is  
100 a required step in library preparation, the problem of working with highly fragmented  
101 samples is obviated. Indeed, Perry and colleagues<sup>31</sup> were able to target and sequence  
102 1.5 megabases of the chimpanzee genome from fecal-derived DNA, using a modified  
103 version of sequence capture, with very low genotyping error rates relative to blood-  
104 derived DNA. More recently, Carpenter et al.<sup>33</sup> reported a method for performing  
105 genome-wide sequence capture from low-quality ancient DNA samples, which  
106 recapitulate many of the challenges posed by non-invasive samples (e.g., highly-  
107 fragmented DNA and low proportions of endogenous DNA).

108         However, while considerable investment in single samples often makes sense in  
109 ancient DNA studies, the low levels of post-capture enrichment associated with

110 currently available protocols are not cost-effective for population studies of non-invasive  
111 samples. Substantially higher rates of enrichment, particularly in non-repetitive regions  
112 of the genome, will be essential to overcome this limitation. In addition, computational  
113 methods for analyzing the resulting data are also required, especially given that  
114 genome-scale sequencing efforts for such samples are likely to produce low coverage  
115 data. For example, current paternity assignment approaches<sup>34–36</sup> were not designed to  
116 deal with uncertain genotypes, an inevitable component of analyzing low coverage  
117 sequencing data. Thus, for capture-based methods to become broadly accessible, the  
118 development of appropriate new computational approaches is also essential.

119 Here, we report an optimized laboratory protocol for genome-wide capture of  
120 endogenous DNA from non-invasively collected samples, combined with a novel  
121 computational approach to reconstruct pedigree links from the resulting data  
122 (implemented in the program *WHODAD*). We validate both our lab methods and  
123 computational tools using non-invasively collected samples from 54 members of an  
124 intensively studied wild baboon population in the Amboseli basin of Kenya<sup>37</sup>. We also  
125 demonstrate the generalizability of our methods to non-invasive samples collected using  
126 different methods from a different baboon species from West Africa. Our protocol is cost  
127 effective, has manageable sample input requirements, yields good capture efficiency for  
128 high complexity, non-repetitive elements, and minimizes the need for extensive PCR  
129 amplification. Importantly, we find that genotype data generated from fecal samples  
130 closely match data from high quality blood-derived DNA samples from the same  
131 individuals, and provide near-perfect information on pedigree relationships even with  
132 extremely low per-sample sequencing coverage (mean = 0.49x genome coverage).

133 Together, these methods will enable population, conservation, and ecological genetic  
134 analyses of natural populations to again take a major leap forward, into the genomic  
135 era. At the same time, they will also introduce valuable new systems to the genomics  
136 community.

137

## 138 RESULTS

139

### 140 *DSN digestion during bait construction increases library complexity*

141 Our protocol relies on *in vitro* transcription of biotinylated RNA baits to capture  
142 host-specific DNA from the mixed pool of host, environmental, and microbial DNA  
143 extracted from non-invasive samples. Similar to Carpenter et al.<sup>33</sup>, RNA baits are  
144 generated from DNA templates obtained from a high quality DNA sample (here, DNA  
145 extracted from blood). This approach avoids the high cost of custom bait synthesis (as  
146 in Gnirke et al.<sup>32</sup> and Perry et al.<sup>31</sup>), but can also produce a bait set that includes a large  
147 proportion of low complexity, repetitive regions. Consequently, reads generated from  
148 captured DNA cannot be uniquely mapped, lowering the protocol's efficiency relative to  
149 using a more diverse bait set. To address this concern, we incorporated a novel duplex  
150 specific nuclease (DSN) digestion in the bait construction step (Fig. S1A; see Methods).  
151 Sequencing the DNA bait templates prior to *in vitro* amplification demonstrates that  
152 including the digestion step reduces the percentage of baits synthesized from low  
153 complexity/highly duplicated regions. Specifically, a 4 hour incubation of sheared DNA  
154 at 68°C followed by a 20 minute DSN digestion in the presence of human Cot-1 greatly  
155 improved the efficiency of capture, producing the highest complexity bait library of the

156 five conditions we tested. Compared to DNA templates from a non-DSN-digested  
157 library, bait templates produced using these conditions reduced the number of reads  
158 mapping to multiple locations by 2.6-fold (from 19.2% to 7.5%; Fig. S2).

159

### 160 *Capture-based enrichment*

161 We validated our full capture protocol (bait construction followed by capture of  
162 endogenous DNA and sequencing of captured fragments) using fecal-derived DNA  
163 (fDNA) samples collected from 54 individually recognized yellow baboons (36 males  
164 and 18 females; Fig. 1) from the Amboseli baboon population, an intensively studied  
165 population in which maternal and paternal pedigree relationships are known for a large  
166 set of individuals<sup>9,37,38</sup>. We produced data for 52 of the samples in two successive  
167 capture efforts: “Capture 1” was conducted on fDNA from 24 baboons, and “Capture 2”  
168 was conducted on fDNA from 28 additional baboons after making multiple  
169 improvements to our initial protocol (changes to the protocol between capture efforts are  
170 described in detail in Table S1; Table S2 provides detailed information on sequencing  
171 coverage and mapping statistics). Data from the remaining two individuals, “LIT” and  
172 “HAP”, were generated to compare the captured fDNA sample with data derived from  
173 sequencing high-quality genomic DNA samples (gDNA) extracted from blood for the  
174 same individuals.



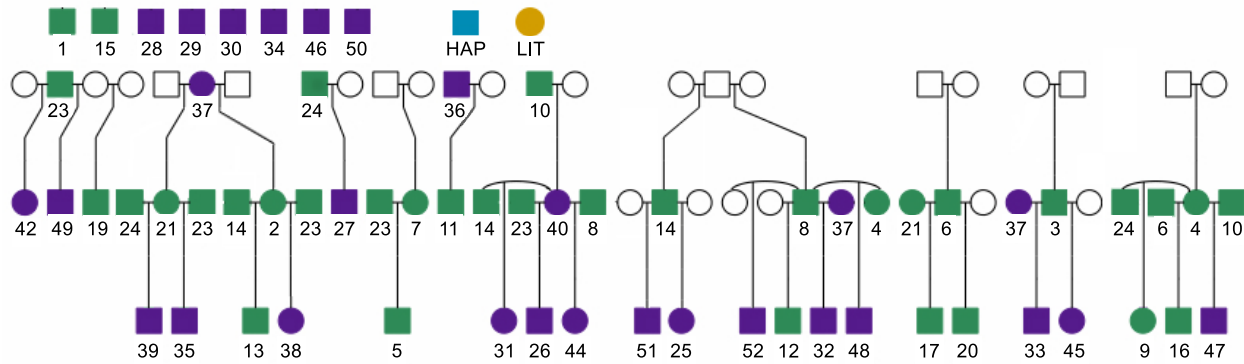


**Figure 1. Pedigree of a subset of baboons monitored by the Amboseli Baboon Research Project.** Samples from both males (squares) and females (circles) were enriched in Capture 1 (green) or Capture 2 (purple). Unfilled circles/squares represent baboons that connect individuals in our pedigree, but who were not sequenced as part of this study. Each sequenced individual is represented by a unique number (below the circle/squares); note that some individuals are repeated in the figure because baboons often produce offspring with multiple mates. The paired fDNA and gDNA samples came from two individuals, HAP (blue) and LIT (orange), who were members of the study population but are not connected to this pedigree.

175

176

177

178

179

180

181

182

183

184

185

186

187

Our protocol (Fig. S1) resulted in substantial enrichment of baboon DNA in the post-capture versus pre-capture samples (see Table S2 for sample-specific details). A mean of 44.56% (range: 10.28-83.17%) of post-capture fragments mapped to the baboon genome, despite starting with pre-capture samples that contained a mean of only 2.04% endogenous baboon DNA, as estimated by qPCR (range 0.19-8.37%). However, in Capture 1 a large proportion of the mapped fragments were identified as PCR duplicates (mean<sub>capture1</sub>=71.97% of mapped fragments, range<sub>capture1</sub>: 51.43-88.46%; Fig. 2A). After removing PCR duplicates, a mean of 9.16% of the post-capture reads in Capture 1 were non-duplicate mappable fragments (range<sub>capture1</sub>=2.23%-23.75%), producing a mean coverage of 0.20x per sample relative to the mappable baboon genome (mean sequencing depth of 5.8 Gb per sample; range<sub>capture1</sub> = 0.04-0.49x; Fig. 2B). These numbers translated to an overall mean fold enrichment of 39.8-

188 fold for mapped reads ( $\text{range}_{\text{capture1}}$ : 8.0-111.8-fold, s.d.=25.2), and 9.6x enrichment of  
189 non-PCR duplicate mapped reads ( $\text{range}_{\text{capture1}}$ :3.9-22.4-fold, s.d.=5.0; Fig. 2C).

190         Based on our results for Capture 1, we made multiple protocol improvements  
191 prior to conducting Capture 2 (Table S1). The improved protocol was twice as effective  
192 on average, resulting in a mean 18-fold enrichment of high quality, analysis-ready reads  
193 and a maximum fold enrichment of close to 40-fold ( $\text{range}_{\text{capture2}}$  = 8.0-39.2-fold; Fig. 2C;  
194 by comparison, methods optimized for ancient DNA achieved a mean of 5.5-fold  
195 enrichment of non-PCR duplicate fragments<sup>33</sup>; Fig. 2A). Specifically, the protocol  
196 changes improved the proportion of non-duplicate mapped fragments by more than  
197 four-fold, from a mean proportion of 9.16% in Capture 1 to a mean proportion of 37.74%  
198 in Capture 2 ( $\text{range}_{\text{capture2}}$ =6.16-68.61%) and reduced the proportion of PCR duplicates  
199 among mapped reads two-fold (from 71.97% in Capture 1 to 36.97% in Capture 2). This  
200 improvement translated to an increase in overall genomic coverage from a mean of  
201 0.20x in Capture 1 to 0.73x in Capture 2 (mean total sequencing of 5.7Gb per sample;  
202  $\text{range}_{\text{capture2}}$  = 0.19-1.24x; Fig. 2B). This improvement in coverage was not explained by  
203 increased sequencing depth in Capture 2 (Table S2). Thus, while we would need to  
204 sequence a pre-capture fDNA sample 50-100 times as deeply as a blood or tissue-  
205 derived sample to produce the same level of coverage, our capture method reduces this  
206 difference to approximately 2 times the sequencing effort. Importantly, our method was  
207 also successful in enriching fDNA samples (n=8) from independent samples collected  
208 from Guinea baboons (*P. papio*; Fig. 2A, Table S2), suggesting that our results are  
209 highly generalizable across different species and storage and extraction methods.

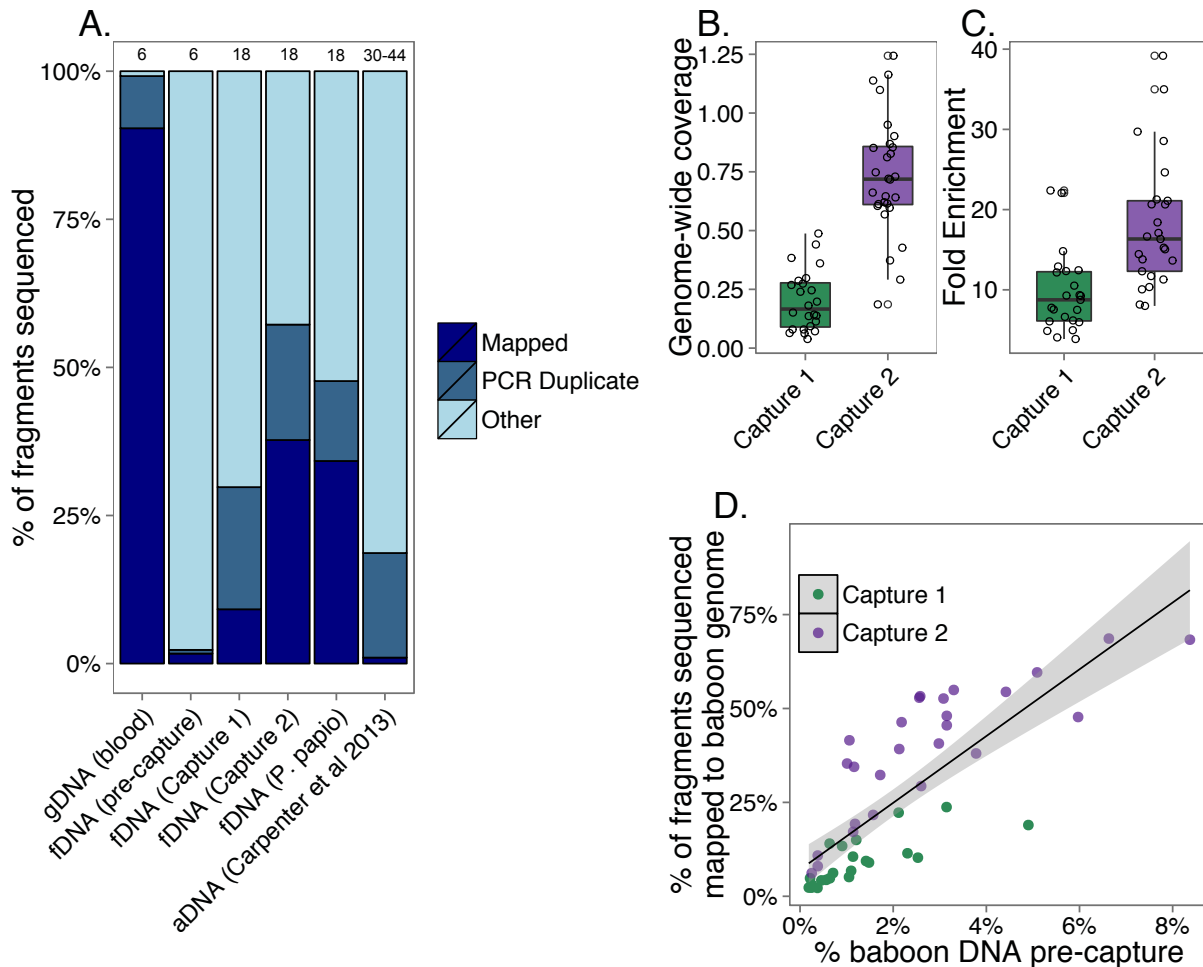


**Figure 2. fDNA enrichment results.** (A) Percent of sequencing reads that mapped to the baboon genome and were not PCR duplicates (“Mapped:” dark blue); mapped and were PCR duplicates (“PCR Duplicate:” blue); or did not map and likely represent environmental or bacterial DNA in the case of fDNA/aDNA and unmappable fragments in the case of gDNA (“Other:” light blue). “gDNA” represents genomic DNA derived from the blood samples for LIT and HAP; “aDNA” represents ancient DNA data from capture-based enrichment reported in Carpenter et al<sup>33</sup>. Numbers above each bar show the total number of PCR cycles used in each protocol. (B) Capture 2 produced significantly greater genome coverage than Capture 1, despite similar number of overall reads generated per sample (two-sample t-test,  $T=9.7$ ,  $p=3.0 \times 10^{-12}$ ). On average in Capture 2, we obtained  $\sim 0.73x$  coverage of the genome with 5.76Gb of sequencing. If all 5.76Gb mapped to the baboon genome as non-PCR duplicates, we would have produced  $\sim 2.2x$  genome-wide coverage. (C) Capture 2 also produced significantly greater fold enrichment of baboon DNA (fold enrichment is measured as % non-duplicate baboon DNA post-capture divided by % baboon DNA pre-capture: two-sample t-test,  $T=4.4$ ,  $p=7.3 \times 10^{-5}$ ). (D) The amount of baboon DNA in the sample pre-capture (% baboon DNA pre-capture, based on qPCR of the single copy *c-myc* gene<sup>39</sup>) is strongly correlated with the percentage of baboon fragments obtained in post-enrichment sequencing (Pearson’s  $r=0.80$ ,  $p=1.0 \times 10^{-11}$ ). However, even samples with low amounts of endogenous DNA (<2%) exhibit substantial fold enrichment using our protocol

( $\text{mean}_{\text{capture1}}=10.60x$ ,  $\text{mean}_{\text{capture2}}=24.82x$ ).

210

### 211 *Sample attributes influencing capture efficiency*

212       The amount of baboon DNA in the pre-capture fDNA sample was the strongest  
213 predictor of enrichment success. Specifically, the percent of baboon DNA pre-capture,  
214 as assessed via qPCR, was positively correlated with the percentage of non-duplicate  
215 fragments mapped post-capture (Fig. 2D;  $T=6.88$ ,  $p=1.72 \times 10^{-8}$ ). Samples from Capture  
216 2 had more pre-capture baboon DNA than samples used in Capture 1 because we  
217 attempted to optimize the input samples based on our initial analyses in Capture 1  
218 (Capture 1 mean = 1.21%, range = 0.19-4.90%; Capture 2 mean = 2.80%, range =  
219 0.25-8.37%). However, even when controlling for this difference, enrichment of samples  
220 from Capture 2 was improved over Capture 1. This pattern is observable whether  
221 assessed using the percent of baboon DNA fragments sequenced post-capture  
222 ( $T_{\text{capture2}}=10.00$ ,  $p=6.76 \times 10^{-13}$ ) or fold enrichment relative to pre-capture amounts  
223 ( $T_{\text{capture2}}=6.89$ ,  $p=1.69 \times 10^{-8}$ ), and could not be explained by differences in the length of  
224 sequence fragments or overall sequencing depth (Fig. S3; Table S2). The amount of  
225 fDNA library used in the capture reaction was also weakly positively correlated with the  
226 percent of baboon DNA fragments sequenced post-capture, after controlling for the  
227 amount of baboon DNA in the pre-capture sample ( $T_{\text{ng\_fDNA\_library}}=2.09$ ,  $p=0.042$ ; Table  
228 S2).

229

### 230 *Library complexity, distribution of reads, and GC content*

231           The post-capture libraries included a higher proportion of PCR duplicates relative  
232 to reads generated from high-quality genomic DNA samples, for which fewer rounds of  
233 PCR amplification were required (PCR duplicate proportion:  $\text{mean}_{\text{fDNA\_capture1}}=69.6\%$ ,  
234  $\text{mean}_{\text{fDNA\_capture2}}=36.8\%$ ,  $\text{mean}_{\text{gDNA}}=11.3\%$  of mapped reads; 18 rounds of PCR in the  
235 capture protocol versus 6 for the high-quality samples). For comparison, this proportion  
236 is much lower than reported for aDNA samples, which go through more rounds of PCR  
237 amplification ( $\text{mean}_{\text{aDNA}}=94.6\%$ ; Fig. 2A and Fig. S4<sup>33</sup>). Despite increases in clonality,  
238 the number of non-duplicate reads continued to increase with increasing sequencing  
239 depth, with the slope of this relationship especially favorable for Capture 2 (Fig. 3).  
240 Thus, deeper sequencing of post-capture libraries should continue to increase genome-  
241 wide coverage, albeit not as efficiently as sequencing blood-derived gDNA samples.

242

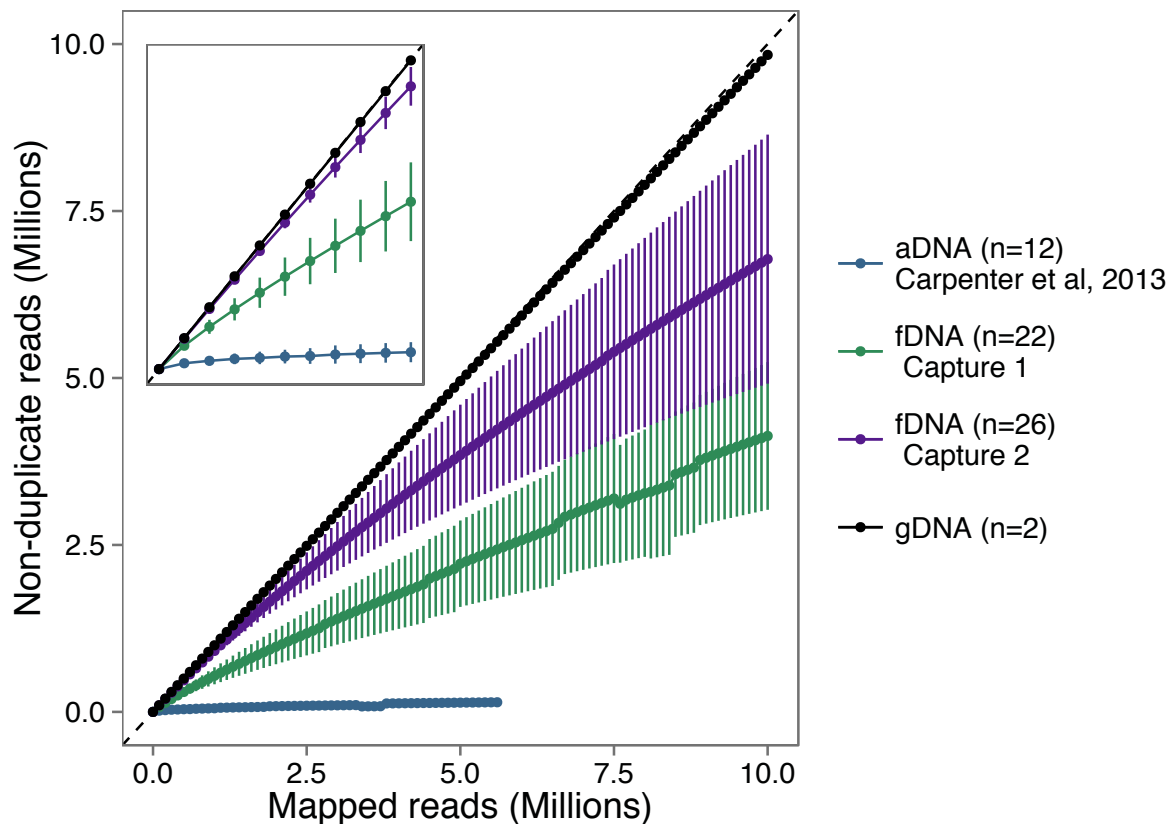


**Figure 3. Increased sequencing effort produces increased numbers of non-duplicate reads.** The number of mapped reads plotted against the number of non-duplicate reads mapped (mean  $\pm$  SD; plotted using the program “preseq”<sup>40</sup>). More complex libraries (i.e., those containing more non-duplicate fragments) have a slope closer to 1 (as in the case of the gDNA libraries), while less complex libraries have a shallower slope and asymptote at a smaller value. The main plot shows the first ten million mapped reads for each sample. The inset shows the same plot for the first million mapped reads.

243 As with other capture-based methods<sup>33,41</sup>, a modest fraction of the mapped  
244 fragments mapped to the mitochondrial genome (mtDNA). When we included all  
245 mapped reads, this fraction was similar in libraries from Capture 1 and Capture 2  
246 (mean<sub>capture1</sub>=6.55%; mean<sub>capture2</sub>=6.73%; Fig. S5A). However, Capture 2 resulted in  
247 significantly more unambiguously non-duplicate mtDNA-mapped reads than Capture 1,  
248 largely due to the paired-end sequencing used in Capture 2 (mean<sub>capture1</sub>=0.47% of all  
249 mapped reads; mean<sub>capture2</sub>=6.46%; Fig. S5B). The higher number of non-duplicate

250 mtDNA reads in Capture 2 thus produced much deeper overall coverage of the  
251 mitochondrial genome (Fig. S5C), despite the fact that the ratio of mtDNA to nuclear  
252 DNA mapped reads was comparable between the two captures (Fig. S5D). Finally, the  
253 distributions of read GC content for post-capture reads using our protocol, the DNA  
254 template for the RNA baits, and aDNA libraries were highly similar (Fig. S6). This  
255 observation suggests that any GC bias relative to the genome appears during bait  
256 construction and/or sequencing, not during the hybridization step.

257

258 *Post-capture fDNA-derived genotype data are consistent with individual identity and*  
259 *independently established pedigree relationships*

260 To assess the accuracy of genotypes called from post-capture fDNA libraries, we  
261 compared genotype data from paired blood-derived gDNA (without capture) and post-  
262 capture fDNA libraries for two individuals, LIT and HAP. Using genotypes for sites that  
263 were called with a genotype quality (GQ) > 20 in both the fDNA and gDNA data sets for  
264 either LIT or HAP, we found that the majority of the genotypes called in both data sets  
265 were concordant (86.5%, or 270,724 of 312,739 sites for the LIT paired samples; 77%,  
266 or 30,948 of 40,132 sites for the HAP paired samples; note that we had lower coverage  
267 for the HAP fecal-derived sample than for the LIT fecal-derived sample). As expected,  
268 the majority of the discordant sites occurred when the low coverage fDNA sample was  
269 called as homozygous and the high coverage gDNA sample was called as  
270 heterozygous (77.7% of discordant LIT<sub>gDNA</sub> heterozygous sites; 74.4% of discordant  
271 HAP<sub>gDNA</sub> heterozygous sites). Importantly, the fDNA genotype captured at least one of  
272 the alleles from the gDNA genotype in 99.8% (LIT) and 99.6% (HAP) of these

273 discordant sites. Thus, even when genotypes called in fDNA and gDNA samples from  
274 the same individual were discordant, they were almost always compatible.

275 Further, we found that genotypes called from the post-capture fDNA libraries  
276 were more similar to the genotypes called from their high-quality gDNA counterparts  
277 than they were to other post-capture fDNA libraries. Specifically,  $k0$  values from  
278 *IcMLkin*<sup>42</sup>, which estimate the probability that two samples share no alleles that are  
279 identical by descent, were much smaller for the  $LIT_{fDNA}$ - $LIT_{gDNA}$  paired samples (0.487)  
280 and  $HAP_{fDNA}$ - $HAP_{gDNA}$  paired samples (0.243) than for  $k0$  values calculated for the two  
281 blood-derived samples when compared to any other fDNA sample ( $k0$  range  $LIT_{fDNA}$   
282 versus other fDNA samples = 0.996 – 1.000;  $Z=849.2$ ,  $p < 10^{-20}$ ;  $k0$  range  $HAP_{fDNA}$   
283 versus other fDNA samples = 0.786 – 0.999;  $Z=10.6$ ,  $p < 10^{-20}$ ; Fig. 4A).

284 For the 48 extended pedigree individuals (Fig. 1, including 8 Amboseli baboons  
285 with no known relatives in the pedigree), we then tested if estimated relatedness values  
286 from *IcMLkin*<sup>42</sup> in the post-capture data were correlated with relatedness values  
287 obtained from the independently constructed pedigree (based on known mother-  
288 offspring relationships and microsatellite-based paternity assignments: see Methods).  
289 Using a filtered set of 127,654 single nucleotide variants (see Methods for filtering  
290 parameters), we found a strong correlation between the two measures (Pearson's  
291  $r=0.73$ ,  $p<10^{-16}$ ; Fig. 4B). This correlation improved further if we imposed thresholds for  
292 the minimum number of sites genotyped in both individuals ("shared sites") in a dyad  
293 (Fig. S7). For example, if we removed all dyads with fewer than 2,000 shared sites (84  
294 of 1,128 dyads, or 7.4%), the correlation between pedigree relatedness and genotype  
295 similarity reached  $r=0.86$  ( $p<10^{-16}$ ).



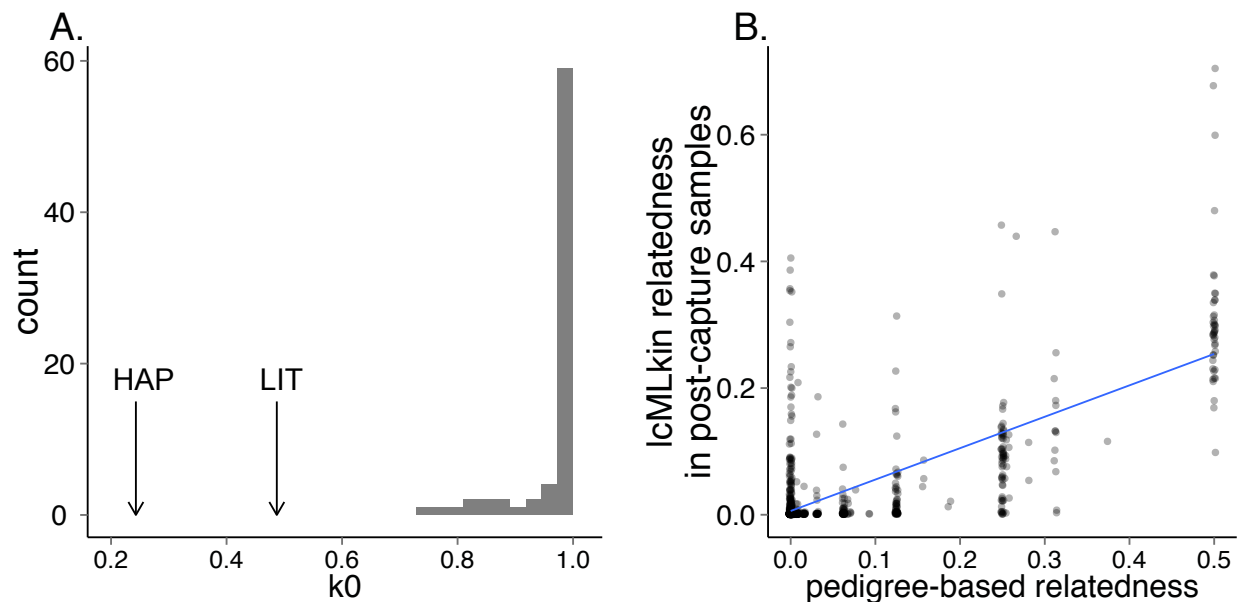


**Figure 4. Post-capture genotype data are consistent with individual identity and pedigree relationships.** (A) The  $k0$  values for the HAP and LIT fDNA-gDNA paired samples (arrows) were significantly lower than the range of  $k0$  values for LIT<sub>fDNA</sub> and HAP<sub>fDNA</sub> versus any other fDNA sample (gray distribution). Lower  $k0$  values reflect increased relatedness (i.e., decreased probability of no IBD sharing). (B) Estimated dyadic relatedness values were correlated with independently obtained pedigree relatedness values calculated using the R package *kinship2* (Sinnwell et al. 2014;  $r=0.73$ ,  $p<10^{-16}$ ). Both  $k0$  and the estimated relatedness values were calculated with *IcMLkin*<sup>42</sup>.

296

297 *Paternity inference using WHODAD*

298 Current methods for assigning paternity (e.g., CERVUS<sup>34,35</sup> and exclusion<sup>36</sup>)

299 assume genotype certainty, such that individuals are assigned a deterministic genotype

300 at each locus (i.e., 0, 1, or 2, or a microsatellite repeat number; while a low level of

301 measurement error, i.e., due to lab handling, can be modeled, this error rate is held

302 constant across genotype calls). This assumption is violated in low coverage

303 sequencing data, in which genotypes are not known with certainty and this uncertainty

304 varies across genotype calls. However, the relative *probabilities* of each genotype can

305 be estimated, given estimated population allele frequencies and sequencing coverage

306 information. To conduct paternity inference and pedigree reconstruction in this context,  
307 we therefore developed a novel approach to integrate information across low coverage  
308 sites, implemented in the program *WHODAD*. Our method has two components. The  
309 first component identifies a top candidate male and tests whether he is significantly  
310 more related to the offspring than any other candidate male, using a p-value criterion.  
311 The second component tests whether the dyadic similarity between the top candidate  
312 and offspring is consistent with a parent-offspring dyad, using posterior probabilities  
313 obtained from a mixture model (see Methods and Fig. S8).

314         Using *WHODAD*, we assigned paternity to all father-offspring pairs ( $n = 27$ )  
315 represented in the independently established extended pedigree in Fig. 1. Note that our  
316 approach represents a particularly conservative test because it departs from the usual  
317 practice of first identifying a likely set of candidate fathers based on demographic and  
318 prior pedigree information (the approach used in producing the pedigree in Fig. 1). For  
319 15 of the 27 offspring, we produced genotype data from the known mother with our  
320 enrichment protocol. *WHODAD* identified the same father as shown in the pedigree in  
321 12 of these 15 trios (80%); in the other 3 trios (20%), no candidate male satisfied  
322 *WHODAD*'s paternity assignment criteria (in all three of these cases, sequencing  
323 coverage was very low for either the pedigree-identified father or offspring: 0.04-0.17x).  
324 For the remaining 12 offspring, we did not generate genotype data using our enrichment  
325 protocol for their mothers (i.e., their mothers were not among the samples run in  
326 Capture 1 or 2). To test all 27 father-offspring dyads together, we therefore re-ran  
327 *WHODAD* excluding maternal genotype information. In this setting, *WHODAD*'s  
328 paternity assignments agreed with the pedigree data in 22 of 27 (81%) cases (Fig. 5).

329 Notably, when the pedigree-identified father was included in the data set, *WHODAD*  
330 never assigned paternity to a different male, whether or not maternal genotype data  
331 were available. Because our method is highly robust to exclusion of maternal genotype  
332 data, we therefore performed all subsequent analyses assuming maternal genotype  
333 data were *not* available. This approach allowed us to evaluate all father-offspring dyads,  
334 and also captures a scenario that may often occur in studies of natural populations.

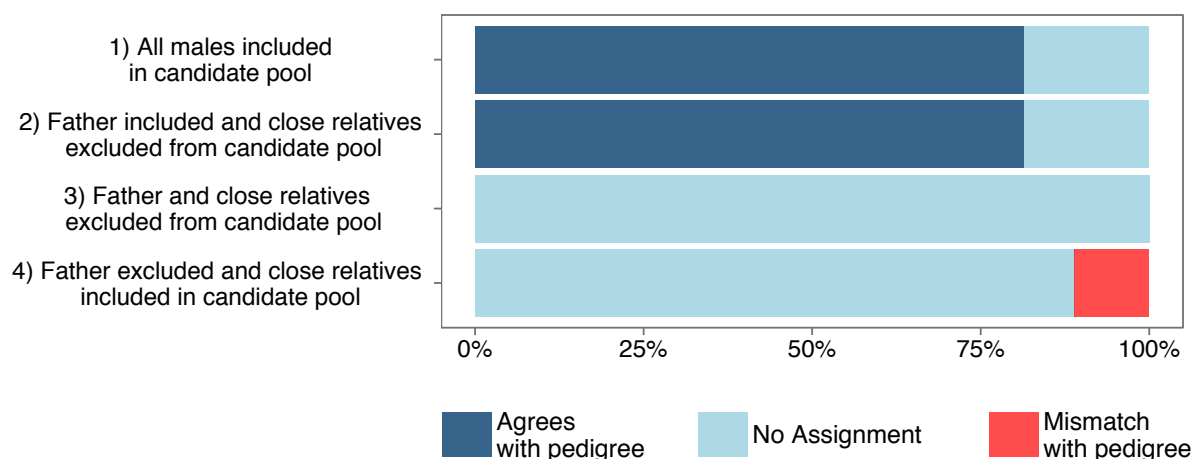


**Figure 5. Paternity inference with *WHODAD* using low coverage genotype calls.**

1) When all males ( $n=34$ ) were included in the pool of candidate fathers (top bar), *WHODAD* assigned paternity to the same father identified in the pedigree for 22 of 27 (81%) of offspring (see assignment criterion in Methods; dark blue). The remaining offspring were not assigned a father based on *WHODAD*'s assignment criteria (5 of 27; light blue). 2) *WHODAD*'s accuracy was identical when we removed all close male relatives of the offspring ( $r \geq 0.25$ ) from the pool of candidate fathers. 3) When we removed all close relatives, including fathers, from the candidate pool, no fathers were assigned, as expected. 4) Finally, when we removed the father from the candidate pool but retained close relatives, our method incorrectly assigned paternity to 11% of offspring (3 of 27; bottom bar). All three incorrectly assigned fathers were closely related to the offspring (in two cases the assigned father was the half-brother of the offspring and in one case the assigned father was the son of the offspring).

335 The presence of close relatives, such as full or half-siblings, can influence the  
336 accuracy of paternity assignment if these close relatives are also included as candidate  
337 fathers<sup>35,44–46</sup>. Thus, to examine how the presence of close male kin influenced the

338 accuracy and confidence of *WHODAD*'s paternity assignments, we conducted three  
339 additional analyses. First, when all close male kin were removed from the candidate list  
340 of potential fathers ( $r \geq 0.25$ ), but the father was retained, our method performed  
341 equivalently to the case when both father and close relatives were in the candidate pool.  
342 Second, when we removed all close male kin *including* the father, none of the best  
343 candidate fathers from the conditional probability analysis (0%) were assigned as  
344 fathers based on *WHODAD*'s assignment criteria (Fig. 5). Third, when we removed the  
345 father from the pool of candidate fathers, but included close male kin, 11% of the best  
346 remaining candidates (3 of 27 cases) were incorrectly assigned as fathers, based on  
347 comparison to the pedigree (Fig. 5). All 3 of these false positives were close male  
348 relatives: in two cases *WHODAD* assigned the half-brother of the offspring as the likely  
349 father, and in one case *WHODAD* assigned the son of the offspring as the likely father.  
350 The best balance between maximizing the number of true positives while minimizing the  
351 number of false positives was achieved by combining both the p-value and mixture  
352 model criteria (see Methods). This approach outperformed either component used alone  
353 (Fig. S9). For example, when all males were included in the candidate pool, the  
354 combined approach resulted in an 81% true positive rate and a 0% false positive rate,  
355 while just using the  $k0$  values in a mixture model resulted in the same true positive rate  
356 (81%), but an additional 11% false positive rate (Fig. S9).

357

## 358 **DISCUSSION**

359 Our capture-based method strongly enriches the proportion of host DNA in low-  
360 quality DNA extracted from feces (fDNA). Our method is the first use of genome-wide

361 enrichment-based capture methods<sup>33,47,48</sup> for non-invasively collected samples, which  
362 represent a major resource for behavioral, conservation, and evolutionary genetic  
363 studies in natural populations. Importantly, our protocol increases efficiency and lowers  
364 cost by reducing the input requirements and number of PCR cycles relative to previous  
365 methods<sup>31</sup> and, in our final protocol, achieves up to 40-fold enrichment of post-capture  
366 endogenous DNA relative to pre-capture levels. We also show, for the first time since  
367 Perry et al<sup>31</sup>, that capture libraries from low-quality samples produce genotype data that  
368 are highly concordant with genotype data derived from high-quality, non-captured  
369 samples from the same individuals.

370         We anticipate that data generated through this protocol could be leveraged for a  
371 wide variety of applications. To illustrate this point for paternity analysis, one of the most  
372 central components of genetic studies in natural populations, we present an  
373 accompanying method, *WHODAD*, that produces results in near-perfect concordance  
374 with an independently constructed pedigree, using low-coverage data generated with  
375 our enrichment protocol (note that the few cases in which assignments could not be  
376 confidently made could readily be addressed with slightly deeper sequencing coverage,  
377 similar to typing more markers in conventional microsatellite analysis). By incorporating  
378 demographic and behavioral data often used to constrain pedigree reconstruction, as  
379 well as prior information about other pedigree links, its performance would be improved  
380 even further. For instance, in reconstructing pedigree links in the Amboseli population,  
381 we generally include only plausible candidates (e.g., we exclude males who were  
382 immature or not yet born at the offspring's conception), not all males with genotype  
383 data, as we did here.

384 Together, these results provide valuable, accessible wet lab and computational  
385 tools for moving studies of difficult-to-sample natural populations forward into the  
386 genomics era. Importantly, our methods can be generalized to produce low complexity  
387 DNA-depleted RNA baits for any species in which at least one high-quality DNA sample  
388 is available (or potentially a closely related species<sup>48</sup>).

389

### 390 *Costs of performing the protocol*

391 At the time of publication, using the same reagents as we used here and sourced  
392 from the same locations, the cost of generating these data is ~\$60/sample (including  
393 sequencing costs). Importantly, our method does not require the commercial synthesis  
394 of targeted capture probes, which is a relatively expensive step for many capture-based  
395 approaches<sup>31,32</sup>. Thus, the majority of the costs are accounted for by the streptavidin-  
396 coated Dynalbeads (\$11/prep), RNA baits (\$5/sample) and High Sensitivity Bioanalyzer  
397 chips for quality control (\$9/sample). Replacing Ampure XP beads with homemade  
398 SPRI beads would reduce the per-sample costs considerably, as would pooling  
399 adapter-ligated fDNA samples prior to hybridization (instead of post-hybridization, as  
400 reported here). For a multiplexed pool of 10 samples, we estimate that using these two  
401 strategies would result in a per-sample cost of ~\$29. Indeed, we have verified that  
402 multiplexing samples prior to hybridization does not result in loss of capture efficiency,  
403 and actually resulted in improved yield of mapped, non-PCR duplicate reads (~61% of  
404 reads; mean of 117-fold enrichment, range = 54.8 – 257.2-fold; Fig. S10A), although it  
405 did result in more uneven coverage of samples sequenced within a pool (Fig. S10B).  
406 Multiplexing also has the advantage of reducing the amounts of input DNA per sample

407 and the number of PCR cycles required for the initial library preparation step. We are  
408 currently pursuing improvements to the protocol along these lines.

409       Based on achieving 40% non-PCR duplicate, mapped reads after capture (the  
410 mean result for Capture 2 samples), we estimate that the sequencing costs of a 1x  
411 genome for baboon (~2.9 Gb) would be about \$200 (based on paired-end, 125-bp  
412 sequencing at \$2,000 per lane and exclusion of PCR duplicates). This cost per sample  
413 is approximately twice the cost of genotyping 14 microsatellites from the same fDNA  
414 sample—the previous strategy for the main study population, the Amboseli baboons<sup>49</sup>—  
415 but provides substantially more genetic information. These estimates will drop further as  
416 the cost of high-throughput sequencing continues to fall, making application of our  
417 approach to whole populations increasingly feasible. Notably, our finding that useful  
418 sequencing reads do not asymptote with deeper sequencing (Fig. 3) also suggests the  
419 feasibility of producing a high-quality, high-coverage genome from such samples if one  
420 were to sequence more deeply than required for the analyses reported here.

421       Finally, to make the current protocol as cost-effective as possible, we  
422 recommend that researchers use qPCR quantification to choose DNA samples with the  
423 highest proportion of host DNA possible—the strongest predictor of the foldchange  
424 enrichment in endogenous DNA post- versus pre-capture (Fig. 2D).

425

#### 426 *Assigning paternity using WHODAD*

427       The lack of available tools for working with low coverage genomic data—  
428 realistically, one of the most likely data types to be produced for studies of natural  
429 populations—represents a major barrier to moving from low-throughput marker

430 genotyping to genome-scale analyses. The pedigree structure of a study population is  
431 fundamental to understanding its genetic structure and social organization. However,  
432 current methods for pedigree reconstruction are unable to cope with high levels of  
433 genotype uncertainty. The approach we have implemented in WHODAD takes this  
434 uncertainty into account, suggesting one simple application for the wet lab methods  
435 presented here. Indeed, our method performed well when compared to an  
436 independently constructed extended pedigree, with its major challenges—differentiating  
437 between close relatives in a candidate pool—comparable to those reported for existing  
438 software<sup>34,35,45,46</sup>. Importantly, while analyses of pedigree structure using previously  
439 available methods are greatly aided by prior knowledge of mother-offspring  
440 relationships<sup>34</sup>, maternal links do not appear to be necessary for WHODAD analyses,  
441 which performs well even when no maternal information is available (Fig. 5; Fig. S8).

442

#### 443 *Conclusions*

444 High-throughput sequencing approaches solve one problem of working with low-  
445 quality, non-invasive samples: the sheared nature of the original samples. Capture  
446 approaches have demonstrated great promise for solving the second major problem—  
447 large proportions of non-endogenous DNA—since the results published by Perry et al  
448 (2010). Motivated by parallel work on ancient DNA, our results help to fulfill this promise  
449 by providing methods to perform cost-effective scaling of sequence capture from non-  
450 invasive samples on a genome-wide scale, coupled with analytical methods to deal with  
451 the resulting data. Our protocols add an important tool to the range of available options  
452 for genetic data generation from such samples. Notably, for questions in which



453 investigators are specifically interested in variants in *a priori*-defined subsets of the  
454 genome (e.g., the exome<sup>50,51</sup>), targeted capture with synthesized baits, followed by  
455 much deeper sequencing, may still be the best option. However, for the many types of  
456 analyses that use genome-scale data (e.g., local ancestry analysis; genome-wide scans  
457 for selection, including in non-coding regions; reconstruction of population demographic  
458 history<sup>20–27,30</sup>), our approach will be more useful, especially as the costs of high-  
459 throughput sequencing continue to fall.

460 Here, we focused specifically on DNA obtained from fecal samples, which are one  
461 of the most commonly collected types of non-invasive samples: they contain information  
462 not only about host genetics, but also about endocrinological parameters<sup>52</sup>, gut  
463 microbiota<sup>53</sup>, parasite burdens<sup>54</sup>, and, as recently demonstrated for human infants, gene  
464 expression levels<sup>55</sup>. The sample banks already available for many natural populations  
465 thus open the door to population and evolutionary genomic studies in species in which  
466 such analyses were previously impossible. As the costs of data generation continue to  
467 fall, and the limiting factor for many studies becomes high quality phenotypic data, we  
468 envision that such studies will rapidly move far beyond the simple analyses of paternity  
469 and pedigree structure reported here.

470

471 **Methods**

472

473 *Bait generation*

474 Similar to Carpenter et al<sup>33</sup>, we use a cost-effective *in vitro* synthesis method  
475 based on T7 RNA polymerase amplification of sheared DNA from a high-quality sample  
476 (Fig. S1A). We extracted genomic DNA from a blood sample collected from an olive  
477 baboon (*Papio anubis*) who was unrelated to any of the individuals in the samples we  
478 wished to enrich. To generate baits, we sheared 5 µg of purified DNA to a mean  
479 fragment size of 150 bp, and then end repaired and A-tailed the fragments using the  
480 KAPA DNA Library Preparation Kit for Illumina Sequencing. We purified the resulting  
481 reaction using a 1.8x ratio of AMPure beads to sample volume.

482 We annealed custom adapters to the A-tailed library by incubating the following  
483 reagents for 15 minutes at 20 °C: 10 µL 5x ligation buffer (KAPA Biosystems); 5 µL  
484 DNA Ligase (KAPA Biosystems); 1 µL 25 µM custom adapter; ≤34 µL of A-tailed DNA;  
485 and H<sub>2</sub>O up to 50µl total volume. The custom adapters we used (EcoOT7dTV: Fwd 5'-  
486 GGAAGGAAGGAAGAGATAATACGACTCACTATAGGGCCTGGT, EcoOT7dTV: Rev  
487 5'-/5Phos/CCAGGCCCTATAGTGAGTCGTATTATCTCTTCCTTCCTTCC) differ from  
488 those used in other protocols<sup>33,47,48</sup>. Specifically, they contained: 1) a T7 RNA  
489 polymerase recognition site; 2) flanking sequence that improves T7 transcription  
490 efficiency<sup>56</sup>; and 3) an EcoO109I restriction enzyme cut site that allowed us to later  
491 cleave off the adapter sequence from T7 amplified RNAs (rather than blocking it, as in  
492 Carpenter et al.<sup>33</sup>).

493 We then digested the purified, adapter-ligated DNA with duplex-specific nuclease  
494 (DSN; Axxora). DSN is a Kamchatka crab-derived enzyme that specifically degrades

495 double-stranded DNA but not single-stranded DNA, allowing us to take advantage of  
496 DNA reassociation kinetics to reduce the representation of repetitive regions in the bait  
497 set (Fig. S2)<sup>57</sup>. We performed DSN digestion in fifteen 2  $\mu$ L aliquots, each mixed with 1  
498  $\mu$ L 4x hybridization buffer (200 mM HEPES pH 7.5; 2 M NaCl; 0.8 mM EDTA) and 1  $\mu$ L  
499 human Cot-1 DNA (1  $\mu$ g/ $\mu$ L). We denatured the DNA by heating to 98°C for 3 minutes,  
500 held the reaction at 68°C for 4 hours, and then added 4  $\mu$ L H<sub>2</sub>O, 1 mL 10x DSN Buffer,  
501 and 1  $\mu$ L DSN (1 U/ $\mu$ L) to the reaction. After 20 minutes of digestion, we stopped the  
502 reaction by adding 5  $\mu$ L 2x DSN Stop Solution (10 mM EDTA) and purified it with 2.4x  
503 AMPure beads.

504         Next, we used Klenow DNA polymerase to blunt end the non-digested DNA,  
505 size-selected for 200 - 300 bp fragments on a 2% agarose gel, and purified the size-  
506 selected fraction using the Zymoclean Gel DNA Recovery Kit (Zymo Research). After  
507 purification the aliquots were PCR amplified for 16 cycles using 25  $\mu$ L 2x HiFi Hot Start  
508 ReadyMix (KAPA Biosystems) and 1  $\mu$ L each of 25  $\mu$ M primers EcoOT7\_PCR1 (5'-  
509 GGAAGGAAGGAAGAGATAATACGACTCACT) and EcoOT7\_PCR2 (5'-  
510 TACGACTCACTATAGGGCCTGGT). Following amplification the bait DNA libraries  
511 were purified using 1.8x AMPure beads and the resulting product was visualized on a  
512 Bioanalyzer DNA 1000 chip (Agilent Technologies).

513         Finally, we *in vitro* transcribed the DNA libraries to construct biotin-tagged RNA  
514 baits using the MEGA Shortscript Kit (Life Technologies) and Biotin-UTP (Illumina).  
515 Briefly, 125-150 nM of DNA baits were incubated at 37°C for 4 hours in the following  
516 reaction: 2  $\mu$ L T7 10x reaction buffer, 2  $\mu$ L each of T7 ATP, GTP, CTP, and UTP  
517 solutions (75 mM), 1  $\mu$ L Biotin-UTP (50 mM), 2  $\mu$ L T7 enzyme mix, and water to 20  $\mu$ L

518 total volume. We then digested the DNA template by adding 1  $\mu$ L TURBO DNase (Life  
519 Technologies) to the reaction and incubating at 37°C for 15 minutes. We purified the  
520 resulting reaction with the MEGAClear Transcription Clean-Up Kit (Life Technologies)  
521 and eluted in a final volume of 70  $\mu$ L. To cleave off the adapter sequence, we digested  
522 the RNA baits with the *EcoO1091* enzyme (NEB). Lastly, the baits were again purified  
523 with the MEGAclean Clean-Up Kit, eluted in 70  $\mu$ L, and quantified on a Bioanalyzer RNA  
524 6000, Eukaryote Total RNA chip (Agilent Technologies).

525

#### 526 *Samples, DNA extraction, and qPCR quantification*

527 Baboon samples were stored in 95% ethanol and fDNA was extracted using the  
528 QIAamp DNA Stool Mini Kit (Qiagen; with slight modifications as described in Alberts et  
529 al.<sup>38</sup>), or using the QIAextractor (protocol available here:  
530 [http://amboselibaboons.nd.edu/assets/84050/alberts\\_fecal\\_genotyping\\_protocol\\_sca.docx](http://amboselibaboons.nd.edu/assets/84050/alberts_fecal_genotyping_protocol_sca.docx))<sup>38</sup>. The majority of the sampled individuals (48 of 54) were either members of a single  
531 extended pedigree or were unrelated males living in the same study population that  
532 were genotyped for inclusion in pedigree building/paternity testing for members of that  
533 pedigree (Fig. 1). For LIT and HAP, gDNA was extracted from blood samples using the  
534 Qiagen Maxi Kit (Qiagen).

536 To assess our protocol's generalizability to samples collected and stored using  
537 different methods, we also extracted fDNA samples from 8 unhabituated Guinea  
538 baboons (*P. papio*) sampled in West Africa. These samples were stored in either 90%  
539 ethanol or soaked in 90% ethanol and then dried using silica beads (i.e., the "two-step"

540 method<sup>58,59</sup>). They were then extracted using either the Qiagen DNA Stool Mini Kit or  
541 the Gen-ial First DNA All Tissue Kit (Table S2).

542 We assessed the proportion of endogenous DNA in each fDNA sample using  
543 qPCR against the *c-myc* gene, as described in Morin et al.<sup>39</sup>.

544

#### 545 *Library preparation*

546 All samples were fragmented to the desired size (200 or 400 base pairs: see  
547 Table S1) using a Bioruptor instrument (Diagenode). Illumina sequencing libraries were  
548 then generated from the fragmented DNA using either the KAPA DNA library kits for  
549 Illumina (Capture 1) or NEBNext DNA Ultra library kit (Capture 2: see Table S1).  
550 Libraries were amplified for 6 PCR cycles prior to capture-based enrichment. Sample-  
551 specific details of library preparation and sequencing results are described in Table S1.  
552 Note that we changed several steps between Capture 1 and Capture 2 based on interim  
553 improvements in the protocol (also detailed in Table S1). Because the methods used in  
554 Capture 2 were ultimately more effective, the updated Capture 2 protocol is described in  
555 the Methods except where explicitly noted.

556

#### 557 *Capture-based enrichment*

558 We modified the capture methods from Gnirke et al<sup>32</sup> and Perry et al<sup>31</sup> (Fig. S1B).  
559 For each capture, we hybridized 121 – 626 ng of the fDNA libraries generated as  
560 described above to the RNA baits. First, we mixed each fDNA library with 2.5  $\mu$ L human  
561 Cot-1 DNA (1 mg/mL), 2.5  $\mu$ L salmon sperm DNA (1 mg/ml), and 0.6  $\mu$ L index-blocking

562 reagent (“IBR”, 50  $\mu$ M). This mixture was incubated for 5 minutes at 95°C followed by  
563 12 minutes at 65°C. Next, we added 13  $\mu$ L of hybridization buffer (10x SSPE, 10x  
564 Denhardt’s solution, 10 mM EDTA, 0.2% SDS, preheated to 65°C), 7  $\mu$ L hybridization  
565 bait mixture (1  $\mu$ L SUPERase-In, 750 ng RNA baits, and water up to a total volume of 7  
566  $\mu$ L, preheated to 65°C) to the fDNA mixture, and incubated the complete mixture at  
567 65°C for 48 hours (see Fig. S11 for comparison of alternative bait concentrations and  
568 incubation times).

569         After incubation, we purified the enriched fDNA sample using 50  $\mu$ L Dynal  
570 MyOne Streptavidin T1 beads (Invitrogen). To do so, the beads were washed a total of  
571 three times with 200  $\mu$ L binding buffer (1 M NaCl, 10 mM Tris-HCl [pH 7.5], 1 mM  
572 EDTA) and resuspended in 200  $\mu$ L of binding buffer. Next, the entire fDNA/RNA  
573 hybridization mix was added to the 200  $\mu$ L Dynal MyOne Streptavidin T1 bead and  
574 binding buffer slurry. We incubated this mixture at room temperature for 30 minutes on  
575 an Eppendorf Thermomixer at 700 rpm. The mixture was placed on a magnetic rack,  
576 the supernatant was discarded, and the beads were washed once with 500  $\mu$ L low  
577 stringency wash buffer (1x SSC, 0.1% SDS) followed by a 15-minute incubation at room  
578 temperature. The beads were then washed three times with 500  $\mu$ L high stringency  
579 wash buffer (0.1x SSC, 0.1% SDS) with a 10 minute room temperature incubation  
580 between each wash. After the final wash, the enriched fDNA fraction was eluted from  
581 the beads with 50  $\mu$ L elution buffer (0.1 M NaOH), transferred to a new tube containing  
582 70  $\mu$ L “neutralization buffer” (1 M Tris-HCl, pH 7.5), purified with 1.8x AMPure beads,  
583 and eluted in a 30  $\mu$ L volume. A final PCR was carried out in a 50  $\mu$ L reaction volume  
584 using 23  $\mu$ L of the post-hybridization fDNA and either: 1) 25  $\mu$ L 2x KAPA High Fidelity

585 master mix and 2  $\mu$ L TruSeq universal primer (Capture 1); or 2) 25  $\mu$ L 2x NEBNext High  
586 Fidelity PCR master mix, 1  $\mu$ L universal PCR primer, and 1  $\mu$ L NEB indexing primer  
587 (Capture 2). After 12 PCR cycles the final reaction was purified with 1x AMPure beads,  
588 eluted in 20  $\mu$ L H<sub>2</sub>O, and visualized on a Bioanalyzer High Sensitivity DNA chip.

589

### 590 *Sequencing and alignment*

591 All high-throughput sequence generation was conducted on the Illumina HiSeq  
592 platform (see Table S1 for sequencing details). The resulting sequencing reads were  
593 mapped to a *de novo* assembly of the *Papio cynocephalus* genome (alignment available  
594 at <https://abrp-genomics.biology.duke.edu/index.php?title=Other-downloads/Pcyn1.0>)  
595 using the default settings of the *bwa mem* alignment algorithm v0.7.4-r385<sup>60</sup>. Duplicate  
596 reads were marked and discarded in subsequent analyses using the “MarkDuplicates”  
597 function in PicardTools (<http://picard.sourceforge.net>). To facilitate comparison across  
598 samples of differing coverage, and because coverage of the gDNA samples was much  
599 higher (~30X) than for the fDNA samples for LIT and HAP (1.4 and 0.27 respectively),  
600 we downsampled the gDNA libraries to 0.73x coverage (the median coverage of  
601 samples in Capture 2) using “DownsampleSam” in PicardTools.

602

### 603 *Comparison sequencing data sets*

604 In several analyses, we compared our capture-based enrichment results to two  
605 independent datasets: i) a previously published capture-based enrichment of ancient  
606 DNA (aDNA) samples (NCBI SRA accession: SRP042225)<sup>33</sup>, and ii) shotgun

607 sequencing from six Capture 1 fDNA samples prior to hybridization (“pre-capture”; Table  
608 1). The aDNA samples were aligned to the human genome (*hg38*) and the pre-capture  
609 fDNA samples were mapped to the *de novo* *P. cynocephalus* genome assembly.

610

#### 611 *Library complexity, distribution of reads, and GC content*

612 We calculated the complexity of each library using two methods. First, we used  
613 the ENCODE Project’s PCR Bottleneck Coefficient (PBC), which calculates the percent  
614 of non-duplicate mapped reads out of the total number of mapped reads<sup>61,62</sup>. The PBC  
615 ranges from 0 to 1, where more complex libraries have higher numbers. Second, we  
616 used the function “c\_curve” from the program *preseq* (v1.0.2) to plot the number of non-  
617 duplicate fragments mapped vs. the number of total mapped fragments<sup>40</sup>. More complex  
618 libraries (i.e., those with fewer duplicate fragments) have a c\_curve slope closer to 1,  
619 meaning that increasing sequencing depth continues to provide novel information. Less  
620 complex libraries have a shallower slope and asymptote at smaller values. Lastly, we  
621 evaluated the GC bias for each sequencing library using Picard Tools’  
622 “CollectGCBiasMetrics” (<http://picard.sourceforge.net>).

623

#### 624 *Sample attributes influencing capture efficiency*

625 To determine the sample attributes that predicted the success of our capture  
626 protocol, we first modeled the relationship between the proportion of non-duplicate  
627 reads that mapped to the baboon genome after capture (our primary measure of  
628 protocol success) and (i) the percent of endogenous baboon DNA in the pre-capture



629 samples; (ii) the amount of fDNA library (ng) that went into the capture; and (iii) whether  
630 the sample was captured using our initial protocol or the second version of the protocol  
631 (i.e., in “Capture 1” or “Capture 2”). Second, we investigated the relationship between  
632 the same three variables and a secondary measure of protocol success, the fold-  
633 change enrichment of baboon DNA in the sample pre- versus post-capture. Pre-capture  
634 concentrations of endogenous DNA in fDNA samples were measured as the  
635 concentration of baboon DNA estimated using qPCR, relative to the concentration of  
636 total DNA estimated using the Qubit High Sensitivity fluorometer (Life Technologies). To  
637 ensure that our qPCR-based measures were well calibrated, we confirmed the  
638 relationship between qPCR-based estimates and pre-capture sequence-based  
639 estimates of endogenous DNA in 6 samples for which both values were available ( $R^2 =$   
640 0.92; Fig. S12). All statistical analyses were carried out in R<sup>63</sup>.

641

#### 642 *Variant calling*

643 We used two different approaches to call variants and genotypes in our sample:  
644 SAMTOOLS<sup>64,65</sup> and the Genome Analysis Toolkit (GATK)<sup>66–68</sup>. In downstream  
645 analyses, we only retained variants that were identified by both methods, a strategy that  
646 produces a higher ratio of true positives to false positives than variants identified by a  
647 single method alone<sup>69</sup>. Duplicate-marked alignments were used as input for both  
648 methods. SAMTOOLS variant calling was carried out using *mpileup* and *bcftools*, with a  
649 maximum allowed read depth (-D) of 100. GATK variant calling was carried out  
650 following the GATK Best Practices for GATK v3.0, for variant calling from DNA-seq. To  
651 minimize potential batch effects introduced by the two capture efforts, we used the

652 following strategy. First, we called genotypes using reads from each capture  
653 independently. Second, we re-called genotypes using reads from both captures  
654 together. Third, we extracted the union set of variants called in steps 1 and 2 for  
655 downstream analysis.

656 Because no reference set of genetic variants is currently publicly available for  
657 baboons, we used a bootstrapping procedure for base quality score recalibration.  
658 Briefly, we performed an initial round of variant calling on read alignments without  
659 quality score recalibration. From this variant call set, we extracted a set of high  
660 confidence variants that passed the following hard filters: quality score  $\geq 100$ ; QD  $< 2.0$ ;  
661 MQ  $< 35.0$ ; FS  $> 60.0$ ; HaplotypeScore  $> 13.0$ ; MQRankSum  $< -12.5$ ; and  
662 ReadPosRankSum  $< -8.0$  (as described in Tung, Zhou, et al.<sup>70</sup>). We then recalibrated  
663 the base quality scores for each alignment using this high-confidence set as the  
664 database of “known variants” and repeated the same variant calling and filtering  
665 procedure for 3 additional rounds. Finally, we identified the intersection set between the  
666 variants called from GATK and SAMTOOLS, respectively, using the *bcftools* function  
667 *isec*<sup>64</sup>. To produce our final call set, we removed all sites that were genotyped in only  
668 one of the capture efforts, had a minor allele frequency of  $< 0.05$ , or were within 10 kb of  
669 one another, using *vcftools*<sup>71</sup>.

670

### 671 *Estimating relatedness*

672 To produce an estimate of relatedness between samples in our pedigree and to  
673 test for concordance between fecal and blood-derived samples for the same individuals,  
674 we used the program *lcMLkin*<sup>42</sup>. *lcMLkin* uses the genotype likelihoods generated by

675 GATK for each genotype call to calculate two measures: (i)  $k_0$ , the probability that two  
676 individuals share no alleles that are identical by descent, and (ii)  $r$ , the coefficient of  
677 relatedness<sup>42</sup>. Several other methods have been developed<sup>72,73</sup> to estimate relatedness  
678 from thousands of SNPs, but *lcMLkin* yielded the best match to pedigree-based  
679 estimates in our data set (Fig. S13).

680 We also compared genotype calls for the matched fecal and blood-derived  
681 samples using GATK's GenotypeConcordance function<sup>68</sup>. This tool allowed us to  
682 determine concordance rates between data sets for different classes of variants (e.g., 0,  
683 1, or 2). For the majority of variant sites, we expected that the genotypes would be  
684 completely concordant (i.e., the same genotype called in the fDNA and gDNA samples  
685 from the same individual). However, for calls reported as discordant, we expected that  
686 most errors would reflect cases in which the low coverage sample was called as  
687 homozygous and the high coverage sample was called as heterozygous, as low read  
688 depth makes observation of both alleles at a heterozygous site less likely.

689

#### 690 *WHODAD: Paternity inference and pedigree reconstruction*

691 Our paternity prediction model is based on a naïve Bayes classifier that takes  
692 advantage of the rules of Mendelian segregation within pedigrees. Using data from all  
693 sites genotyped in a potential father-mother-offspring trio or, when the mother is not  
694 genotyped, all sites genotyped in a potential father-offspring dyad, it estimates the  
695 posterior probability that a potential candidate is the true father of a given offspring.

696 Our approach can be broken into three steps (Fig. S8). First, we estimate, for  
697 each candidate male, the conditional probability that he is the true father of a given

698 offspring, given the genotype data for the candidate, offspring, and mother, if known  
699 (below we show the case in which genotype information is available for the mother, but  
700 the model is similar when maternal genotype information is missing). Second, we assign  
701 a p-value for the top candidate male from the first step, for the null hypothesis that he is  
702 *not* more related to the focal offspring than the other candidates tested. Third, we  
703 calculate the probability that the genotype data for the top candidate and offspring are  
704 consistent with a true parent-offspring relationship, using a mixture model. Steps (ii) and  
705 (iii) perform subtly different functions in our analysis: (ii) tests that the top candidate is  
706 significantly more related to the offspring than any other candidate, whereas (iii) tests  
707 that the dyadic similarity between the candidate and the offspring look as expected for  
708 parent-offspring dyads. We have found that combining both approaches is key to  
709 detecting true positive fathers while minimizing false positive calls that can occur when  
710 true fathers are not in the pool of genotyped candidates (Fig. S8).

711 *Step 1: estimating conditional probabilities for each trio.* For a given offspring or  
712 mother-offspring dyad, our goal is to infer the true genetic father from a pool of  $n$   
713 candidates. For the  $i^{\text{th}}$  candidate, we use data for the  $L_i$  variants for which we have  
714 genotype information for the known mother-offspring dyad and for the candidate father.  
715 Assuming the true father is present in the candidate pool (i.e., he has been genotyped),  
716 the probability that the  $i^{\text{th}}$  potential candidate is the father is:

$$P(F_i|M, O) = P(F_i, M, O) / \left( \sum_{k=1}^n P(F_k, M, O) \right) \quad (1)$$

717 where  $P(F_i|M, O)$  denotes the probability that the candidate is the father, conditional on  
718 the (known) mother-offspring dyad;  $P(F_i, M, O)$  denotes the joint probability of the whole  
719 trio; and  $\sum_{k=1}^n P(F_k, M, O)$  is the sum of the joint probabilities of all possible trios evaluated

720 in the analysis. In practice, we normalize these conditional probabilities to take into  
721 account differences in the number of variants evaluated for each trio by taking the  $L_i^{\text{th}}$   
722 root:

$$P(F_i|M, O) \approx P(F_i, M, O)^{1/L_i} / \left( \sum_{k=1}^n P(F_k, M, O)^{1/L_k} \right) \quad (1a)$$

723 Each joint probability can be calculated in turn as:

$$P(F_i, M, O) = \sum_{f, m, o} P(F_i, M, O, f, m, o) = \sum_{f, m, o} \prod_{j=1}^{L_i} P(F_i, M, O, f_{ij}, m_j, o_j) \quad (2)$$

724 where  $m_j$ ,  $f_{ij}$  and  $o_j$  represent the genotype data for the  $j^{\text{th}}$  variant of the mother, the  
725 candidate father, and the offspring, respectively. Genotypes take values in  $\{0, 1, 2\}$  (i.e.,  
726 the number of copies of the reference allele at each individual-site combination).  
727 Importantly, although equation (2) unrealistically assumes independence across loci,  
728 this assumption does not change the relative order of trio joint probabilities.

729 The probability  $P(F_i, M, O, f_{ij}, m_j, o_j)$  for each locus can be further decomposed as:

$$P(F_i, M, O, f_{ij}, m_j, o_j) \propto P(o_j|m_j, f_{ij}) \frac{P(f_{ij}|F_i)P(m_j|M)P(o_j|O)}{P(o_j)} \quad (3)$$

730 where we take genotype uncertainty into account by using GATK's genotype  
731 probabilities to calculate the conditional genotype probabilities for  $P(f_{ij}|F_i)$ ,  $P(m_j|M)$ , and  
732  $P(o_j|O)$  over all possible genotype values at each site-individual combination (i.e., the  
733 probabilities that each genotype is 0, 1, or 2, which sum to 1). We also ignore the  
734 scaling constant  $P(F_i)P(M)P(O)$  because it cancels out in the numerator and  
735 denominator of (1). The marginal probability of the offspring's genotype,  $P(o_j)$ , is  
736 calculated from the minor allele frequency of the variant in the population. Finally, the  
737 conditional probability  $P(o_j|m_j, f_{ij})$  is based on the rules of Mendelian transmission (e.g.,

738 Marshall et al., 1998). Due to genotype uncertainty in low coverage data, the values of  
739  $P(F_i|M, O)$  are small. However, the highest value is usually assigned to the most likely  
740 father (based on comparison to the pedigree; see Results) and we can directly assess  
741 the strength of the relative evidence for the top candidate versus other candidates in  
742 Step 2 by calibrating these values against permuted data.

743 *Step 2: calculating resampling-based p-values.* To compute p-values for each  
744 paternity assignment, candidates are ranked based on their conditional probability  
745  $P(F_i|M, O)$  of being the true father. The log ratio of conditional probabilities between the  
746 highest probability father and the second best candidate is the test statistic:

$$r = \log \left( \frac{P(F_{best}|M, O)}{P(F_{second}|M, O)} \right) \quad (4)$$

747 To assess significance for  $r$ , we then simulate genotype data for a set of  $n$   
748 unrelated candidate fathers based on allele frequency information for each locus in the  
749 analysis and sequence coverage information for the real candidates, at each of the loci  
750 for which they were genotyped in the true data set. Specifically, for each locus-  
751 simulated unrelated candidate combination,  $f_{ij}$ , where  $i$  indexes a (real) candidate male  
752 and  $j$  indexes the locus, we simulate a vector of genotype probabilities for the candidate  
753 father,  $(f_{ij0}, f_{ij1}, f_{ij2})$ , which sum to 1. The number of probability vectors simulated for  
754 each candidate is based on the number and identity of the loci observed in the real  
755 data. For example, if the top candidate in the real data was evaluated based on 10,000  
756 sites, we would simulate an unrelated male with genotype vector probabilities simulated  
757 for each of those 10,000 sites; if the second best candidate was evaluated at 9,000  
758 sites, we would simulate an unrelated male with genotype vector probabilities simulated

759 for each of those 9,000 sites; and so on. The variant sets for different simulated  
760 candidates need not be identical, and are in fact highly unlikely to be so in practice.

761 To simulate each vector, we draw values from a Dirichlet distribution (i.e., a  
762 distribution on probability vectors that sum to one). In principle, the Dirichlet distribution  
763 for each biallelic site could be parameterized by the genotype frequencies for each of  
764 the three potential genotype values,  $Dir(\pi_{j0}, \pi_{j1}, \pi_{j2})$ , with genotype frequencies equal to  
765 the Hardy-Weinberg expected values based on the allele frequency of the reference  
766 allele (i.e.,  $p^2$ ,  $2p(1-p)$ ,  $(1-p)^2$ , with  $p$  estimated from the data). However, the low  
767 coverage in our data introduces additional noise into this sampling problem, so we  
768 instead draw values from the following Dirichlet distribution:

$$(f_{ij0}, f_{ij1}, f_{ij2}) \sim Dir(\kappa c_{ij}(\pi_{j0}, \pi_{j1}, \pi_{j2})) \quad (5)$$

769 where  $c_{ij}$  is the read depth (coverage) for the site in (true) candidate father  $i$ , and  $\kappa$  is a  
770 concentration parameter common to all sites and candidate fathers, estimated from the  
771 real data using the method of moments.  $\kappa$  can be thought of as a scaling factor for the  
772 effect of coverage on variance in  $(f_{ij0}, f_{ij1}, f_{ij2})$ . To make the simulations as realistic as  
773 possible, all parameters are estimated from the real data as follows:

$$\pi_{jl} = E(f_{ijl}) \quad (6)$$

774 where the expectation is based on the allele frequencies for the reference allele  
775 estimated across all individuals, for each locus  $j$  and genotype  $l$  combination, and:

$$\kappa = \frac{E(f_{ijl}) - E(f_{ijl}^2)}{E(c_{ij} f_{ijl}^2) - E^2(c_{ij} f_{ijl})} \quad (7)$$

776 where the expectations are based on the allele frequencies (as above) across all  
777 individuals and loci, and across all 3 possible genotype values (0, 1, and 2) for each  
778 locus-individual combination. Our estimates for  $\pi_{ij}$  and  $\kappa$  are based on the observed  
779 average values from the data, which approximate the expected value.

780 After simulating genotype data for each candidate male as if he were unrelated to  
781 the focal offspring, we can obtain a new value of  $r$  (equation 4) from the simulated data.  
782 By repeating this procedure  $s$  times, we can compute a p-value for the hypothesis that  
783 the best candidate in the true data is no more related to the focal offspring than any  
784 other candidate in the data set. This p-value is equal to the proportion of times the  
785 simulated test statistics exceed the observed test statistic. It intuitively corresponds to  
786 the probability of seeing a gap as large as the true gap between the conditional  
787 probabilities for the best and second best candidates, if all candidates were in fact  
788 unrelated (or equally related) to the focal offspring.

789 *Step 3: estimating the posterior probability of paternity.* WHODAD's inference  
790 method, like other paternity inference methods (e.g., CERVUS<sup>34,35</sup>), can falsely assign  
791 paternity to a close relative if the true father is not included in the pool of potential  
792 fathers. Such false positives arise because these methods do not actually test the  
793 hypothesis that the assigned father is the true father, but rather whether the assigned  
794 father is significantly more closely related to the focal offspring than other candidates in  
795 the pool. A more direct method would be to test the probability of observing the data for  
796 a father-offspring dyad (or father-mother-offspring trio) under the *alternative* hypothesis  
797 that the assigned father is the true father. Testing the alternative hypothesis is non-  
798 trivial with low-coverage data, and by itself can also yield incorrect inferences (Fig. S9).



799 However, in combination with the resampling-based p-values described above, it can  
800 improve paternity assignments.

801 To estimate the probability of the data given the best candidate-offspring dyad,  
802 we take advantage of the fact that dyadic measures of genotype similarity, relatedness,  
803 or other estimates of identity-by-descent should differ for true parent-offspring pairs  
804 compared to all other dyads (except for full sibs). By utilizing the many dyadic values in  
805 a data set of mothers, offspring, and candidate fathers, we should therefore be able to  
806 distinguish father-offspring dyads from dyads involving other relatives or unrelated pairs.  
807 Notably, this method allows us to use dyadic values for mother-offspring pairs to  
808 maximum effect.

809 We use a normal mixture clustering approach and the  $k0$  value from the R  
810 package *lcMLkin*, where low  $k0$  values predict high pedigree relatedness (other  
811 measures of dyadic relatedness could be substituted, but the  $k0$  values produced the  
812 best correlation with known pedigree-based measures of relatedness in our sample:  
813 Fig. S13). We denote  $y_b$  as the vector of logit-transformed  $k0$  measurements for the  
814 best candidate-offspring dyads for all tested father-offspring dyads;  $y_1$  as the vector of  
815 logit( $k0$ ) measurements for all known mother-offspring dyads, if any are present ( $y_1$  can  
816 be an empty vector if no mother-offspring dyads were sampled); and  $y_0$  as the vector of  
817 logit( $k0$ ) measurements for all other dyads. Thus,  $y_0$  captures the distribution of logit( $k0$ )  
818 values for non-parent-offspring dyads;  $y_1$  captures the distribution of logit( $k0$ ) values for  
819 known parent-offspring dyads; and  $y_b$  contains a mixture of logit( $k0$ ) values for both true  
820 parent-offspring dyads and non-parent-offspring dyads.

821 We first work only with  $y_0$ , and use a mixture model approach to assign the  
822  $\text{logit}(k_0)$  value for each dyad  $i$  into one of  $K$  component normal distributions (fit using the  
823 *mixtools* function in R, with a default value of  $K=5$ ). Components with lower mean  
824 values for  $k_0$  can be thought of as capturing the distribution of  $\text{logit}(k_0)$  values for highly  
825 related dyads (e.g., half-siblings), whereas components with high mean values capture  
826 distantly related or unrelated dyads (if relatedness coefficients were used instead of  $k_0$ ,  
827 this direction would be reversed: low values would correspond to distantly related dyads  
828 instead). For  $y_1$ , all dyads are from the same relatedness category (mother-offspring),  
829 so  $\text{logit}(k_0)$  values in  $y_1$  can be modeled by a single distribution parameterized by a  
830 mean and a variance. Finally, for  $y_b$ , values of  $\text{logit}(k_0)$  can be assumed to be drawn  
831 from either the distribution on  $y_1$  or from one of the distributions (likely one with a low  
832 mean value) in the mixture model for  $y_0$ :

$$y_{bi} \sim \pi N(\mu, \sigma^2) + (1 - \pi) N(\mu_i, \sigma_i^2) \quad (8)$$

833 where for the  $i$ th individual in  $y_b$ ,  $\mu_i$  and  $\sigma_i^2$  are the mean and variance for one of the  
834 distributions in the mixture model of  $y_0$ ;  $\mu$  and  $\sigma^2$  are the mean and variance for the  
835 distribution on  $y_1$ ; and  $\pi$  is the probability that a value in  $y_b$  belongs to the parent-  
836 offspring distribution or one of the distributions fit in the mixture model for other dyads.  
837 To infer these parameters, for each dyad in  $y_b$ , we assign  $\mu_i, \sigma_i^2$  to the mean and  
838 variance of the mostly likely normal component by evaluating the likelihood under all  $K$   
839 components. We then combine  $y_1$  and  $y_b$  to jointly infer  $\pi, \mu, \sigma^2$  in equation (8).

840 Finally, we introduce a latent indicator variable  $z_{bi}$  for each dyad to indicate if the  
841  $i^{\text{th}}$  dyad in  $y_b$  is a true father-offspring dyad. The probability of being a true father-  
842 offspring dyad, or  $P(z_{bi}=1)$ , becomes the final statistic used to assess our paternity

843 assignments. To infer  $P(z_{bi}=1)$ , we use an expectation-maximization algorithm (see  
844 Supplementary Methods for detailed information about the EM steps). WHODAD  
845 considers a male as the likely true father of a focal offspring if he was (i) the candidate  
846 with the highest conditional probability of paternity; (ii) assigned a p-value from our  
847 simulations  $< 0.05$ ; and (iii)  $P(z_{bi}=1) > 0.9$ .

848

#### 849 *Testing the accuracy of paternity assignment using WHODAD*

850 We assigned paternity using the methods detailed above for all previously  
851 identified father-offspring pairs ( $n = 27$ ) in the Amboseli pedigree (Fig. 1). This pedigree  
852 was constructed using a combination of observational life history data on female  
853 pregnancies and infant care (to infer maternal-offspring dyads), demographic data to  
854 identify possible candidate fathers, and microsatellite genotyping data analyzed in the  
855 program CERVUS (with confidence  $>95\%$ ; see Alberts et al.<sup>38</sup> for additional detail).

856 Our data set contained maternal genotype information derived from the fecal  
857 enrichment protocol for 15 of these individuals (56%). We first used *WHODAD* to assign  
858 paternity for these 15 offspring while incorporating the genotype data from their  
859 mothers. To assess the accuracy of *WHODAD* in the absence of maternal genotype  
860 data, we then repeated the paternity analysis for the same 15 offspring without including  
861 the mother's genotype. For this analysis, we were also able to include the 12 additional  
862 offspring for whom we did not have genotype data from the mother, but had genotype  
863 data from the known father ( $n=27$ ).

864 To examine how the presence of close male kin influenced the accuracy and  
865 confidence of *WHODAD*'s paternity assignments, we conducted three additional

866 analyses. First, to assess the accuracy of *WHODAD* when the pedigree-assigned father  
867 is the only close male relative present, we removed all close relatives of the offspring  
868 except the father ( $r \geq 0.25$ , e.g., grandfathers, half-sibling or full-sibling brothers) from the  
869 pool of potential fathers. Second, to test if *WHODAD* assigned a father with high  
870 confidence even when no close relatives were present, we removed all close male  
871 relatives, including the pedigree-assigned father, from the pool of candidate males.  
872 Third, to assess the risk of confidently (but erroneously) assigning a close male relative  
873 as the likely father when the pedigree-assigned father was not genotyped, we removed  
874 the father from the pool of potential fathers. For all *WHODAD* analyses we report  
875 assignment accuracy based on whether the father was identified by *WHODAD* with a p-  
876 value less than 0.05 and a  $P(z_{bi}=1) > 0.90$ . Offspring were not assigned a father (“no  
877 assignment”) when the best candidate male was identified with a p-value  $> 0.05$  or a  
878  $P(z_{bi}=1) < 0.90$ .

879

880

881 **ACKNOWLEDGEMENTS**

882           We would like to thank the Kenya Wildlife Service, Institute of Primate Research,  
883 National Museums of Kenya, National Council for Science and Technology, members of  
884 the Amboseli-Longido pastoralist communities, Tortilis Camp, and Ker & Downey  
885 Safaris for their assistance in Kenya. We also thank Jeanne Altmann and Elizabeth  
886 Archie for their generous support and access to the Amboseli Baboon Research Project  
887 data set and samples; Raphael Mututua, Serah Sayialel, Kinyua Warutere, Mercy  
888 Akinyi, Tim Wango, and Vivian Oudu for invaluable assistance with the Amboseli  
889 baboon sample collection; Emily McLean for assistance in identifying samples from the  
890 extended pedigree; and Tauras Vilgalys for assistance in drawing the pedigree. For  
891 access to the Guinea baboon samples, we thank Julia Fischer, Dietmar Zinner and José  
892 Carlos Brito; the Wild Chimpanzee Foundation for logistical support in Guinea; and the  
893 Ministère de l'Environnement et de la Protection de la Nature and the Direction des Parcs  
894 Nationaux in Senegal, the Opération du Parc National de la Boucle du Baoulé and the  
895 Ministère de l'Environnement et de l'Assainissement in Mali, the Office Guinéen de la  
896 Diversité Biologique et des Aires Protégées and the Ministère de L'Environnement, des  
897 Eaux et Forêts in Guinea, and the Ministère Délégué auprès du Premier Ministre,  
898 Chargé de l'Environnement et du Développement Durable in Mauritania. Finally, we  
899 thank PJ Perry, Luis Barreiro, Greg Crawford, Tim Reddy, and members of the Alberts  
900 and Tung labs for their feedback on earlier versions of this work. This work was  
901 supported by National Science Foundation grants DEB-1405308 (to JT) and SMA-  
902 1306134 (to JT and NSM). GHK was supported by the German Academic Exchange

903 Service (DAAD), the Christiane-Nüsslein-Volhard Foundation, The Leakey Foundation,  
904 and the German Primate Center. XZ was supported by a grant from the Foundation for  
905 the National Institutes of Health through the Accelerating Medicines Partnership  
906 BOEH15AMP.  
907

908 DATA ACCESSIBILITY:

909 All resequencing data sets reported in this manuscript will be deposited in the NCBI  
910 Short Read Archive (SRA) upon acceptance. A reviewer URL for the metadata and run  
911 info for these data sets is available at [ftp://ftp-  
912 trace.ncbi.nlm.nih.gov/sra/review/SRP064514\\_20151007\\_093529\\_a3f2a910685f5b07f5  
913 f45a5fc1fdb389](ftp://ftp-trace.ncbi.nlm.nih.gov/sra/review/SRP064514_20151007_093529_a3f2a910685f5b07f5f45a5fc1fdb389).

914

915

916 AUTHOR CONTRIBUTIONS:

917 JT, NSM, SM, and XZ conceived and designed the research. MLY, AOS, JBG, GHK,  
918 and NSM performed all laboratory experiments. SAS, JT, and JDW provided the  
919 genome assembly. WHM, SM and XZ developed the computational methods. WHM and  
920 XZ implemented the software. NSM, JT, and XZ analyzed the data. SCA and GHK  
921 provided samples, reagents, and logistical support. NSM, JT, and XZ wrote the  
922 manuscript with input from all of the coauthors.

923

924 COMPETING FINANCIAL INTERESTS:

925 The authors declare no competing financial interests.

926

927 **References Cited**

- 928 1. Höss, M., Kohn, M., Pääbo, S., Knauer, F. & Schröder, W. Excrement analysis by  
929 PCR. *Nature* **359**, 199–199 (1992).  
930
- 931 2. Ashley, M. & Dow, B. The use of microsatellite analysis in population biology:  
932 background, methods and potential applications. *Mol. Ecol. Evol. approaches*  
933 *Appl.* **69**, 185–201 (1994).  
934
- 935 3. Clifford, S. L. *et al.* Mitochondrial DNA phylogeography of western lowland gorillas  
936 (*Gorilla gorilla gorilla*). *Mol. Ecol.* **13**, 1551–65, 1567 (2004).  
937
- 938 4. Nyakaana, S., Arctander, P. & Siegismund, H. R. Population structure of the  
939 African savannah elephant inferred from mitochondrial control region sequences  
940 and nuclear microsatellite loci. *Heredity (Edinb)*. **89**, 90–8 (2002).  
941
- 942 5. Kohn, M. & Knauer, F. Phylogeography of Brown Bears in Europe and  
943 Excremental PCR: The New Tool in the Genetic Analysis of Animals in the Wild.  
944 *Ursus* **10**, Phylogeography of brown bears in Europe and excrem (1998).  
945
- 946 6. Charpentier, M. J. E. *et al.* Genetic structure in a dynamic baboon hybrid zone  
947 corroborates behavioural observations in a hybrid population. *Mol. Ecol.* **21**, 715–  
948 731 (2012).  
949
- 950 7. Sacks, B. N., Moore, M., Statham, M. J. & Wittmer, H. U. A restricted hybrid zone  
951 between native and introduced red fox (*Vulpes vulpes*) populations suggests  
952 reproductive barriers and competitive exclusion. *Mol. Ecol.* **20**, 326–341 (2011).  
953
- 954 8. Pérez, T. *et al.* Evidence for improved connectivity between Cantabrian brown  
955 bear subpopulations. *Ursus* **21**, 104–108 (2010).  
956
- 957 9. Buchan, J. C., Alberts, S. C., Silk, J. B. & Altmann, J. True paternal care in a  
958 multi-male primate society. *Nature* **425**, 179–181 (2003).  
959
- 960 10. Smith, K., Alberts, S. C. & Altmann, J. Wild female baboons bias their social  
961 behaviour towards paternal half-sisters. *Proc. R. Soc. B Biol. Sci.* **270**, 503  
962 (2003).



963

964 11. Archie, E. A. *et al.* Behavioural inbreeding avoidance in wild African elephants.  
965 *Mol. Ecol.* **16**, 4138–48 (2007).

966

967 12. Gottelli, D., Wang, J., Bashir, S. & Durant, S. M. Genetic analysis reveals  
968 promiscuity among female cheetahs. *Proc. R. Soc. B Biol. Sci.* **274**, 1993–2001  
969 (2007).

970

971 13. Mondol, S. *et al.* Evaluation of non-invasive genetic sampling methods for  
972 estimating tiger population size. *Biol. Conserv.* **142**, 2350–2360 (2009).

973

974 14. Nagata, J., Aramilev, V. V., Belozor, A., Sugimoto, T. & McCullough, D. R. Fecal  
975 genetic analysis using PCR-RFLP of cytochrome b to identify sympatric  
976 carnivores, the tiger *Panthera tigris* and the leopard *Panthera pardus*, in far  
977 eastern Russia. *Conserv. Genet.* **6**, 863–866 (2005).

978

979 15. Idaghdour, Y., Broderick, D. & Korrida, A. Faeces as a source of DNA for  
980 molecular studies in a threatened population of great bustards. *Conserv. Genet.*  
981 **4**, 789–792 (2003).

982

983 16. Rudnick, J. A., Katzner, T. E., Bragin, E. A. & DeWoody, J. A. A non-invasive  
984 genetic evaluation of population size, natal philopatry, and roosting behavior of  
985 non-breeding eastern imperial eagles (*Aquila heliaca*) in central Asia. *Conserv.*  
986 *Genet.* **9**, 667–676 (2007).

987

988 17. Valière, N. *et al.* Long-distance wolf recolonization of France and Switzerland  
989 inferred from non-invasive genetic sampling over a period of 10 years. *Anim.*  
990 *Conserv.* **6**, 83–92 (2003).

991

992 18. Taberlet, P., Waits, L. & Luikart, G. Noninvasive genetic sampling: look before  
993 you leap. *Trends Ecol. Evol.* **14**, 323–327 (1999).

994

995 19. Gagneux, P., Boesch, C. & Woodruff, D. S. Microsatellite scoring errors  
996 associated with noninvasive genotyping based on nuclear DNA amplified from  
997 shed hair. *Mol. Ecol.* **6**, 861–8 (1997).

998

- 999 20. Li, H. & Durbin, R. Inference of human population history from individual whole-  
1000 genome sequences. *Nature* (2011).  
1001
- 1002 21. Sabeti, P., Reich, D. & Higgins, J. Detecting recent positive selection in the  
1003 human genome from haplotype structure. *Nature* (2002).  
1004
- 1005 22. Price, A., Tandon, A., Patterson, N. & Barnes, K. Sensitive detection of  
1006 chromosomal segments of distinct ancestry in admixed populations. *PLoS Genet*  
1007 (2009).  
1008
- 1009 23. Sankararaman, S. & Sridhar, S. Estimating local ancestry in admixed populations.  
1010 *Am. J. ...* (2008).  
1011
- 1012 24. Yang, J. *et al.* Genome partitioning of genetic variation for complex traits using  
1013 common SNPs. *Nat. Genet.* **43**, 519–25 (2011).  
1014
- 1015 25. Ma, Y. *et al.* Accurate inference of local phased ancestry of modern admixed  
1016 populations. *Sci. Rep.* **4**, 5800 (2014).  
1017
- 1018 26. Huang, B., Amos, C. & Lin, D. Detecting haplotype effects in genomewide  
1019 association studies. *Genet. Epidemiol.* (2007).  
1020
- 1021 27. Li, Y., Sung, W. & Liu, J. Association mapping via regularized regression analysis  
1022 of single-nucleotide-polymorphism haplotypes in variable-sized sliding windows.  
1023 *Am. J. Hum. Genet.* (2007).  
1024
- 1025 28. Purcell, S. *et al.* PLINK: A Tool Set for Whole-Genome Association and  
1026 Population-Based Linkage Analyses. *Am. J. Hum. Genet.* **81**, (2007).  
1027
- 1028 29. Visscher, P. M. Whole genome approaches to quantitative genetics. *Genetica*  
1029 **136**, 351–358 (2009).  
1030
- 1031 30. Durand, E. Y., Patterson, N., Reich, D. & Slatkin, M. Testing for ancient admixture  
1032 between closely related populations. *Mol. Biol. Evol.* **28**, 2239–2252 (2011).  
1033

- 1034 31. Perry, G. H., Marioni, J. C., Melsted, P. & Gilad, Y. Genomic-scale capture and  
1035 sequencing of endogenous DNA from feces. *Mol. Ecol.* **19**, 5332–44 (2010).  
1036
- 1037 32. Gnirke, A. *et al.* Solution hybrid selection with ultra-long oligonucleotides for  
1038 massively parallel targeted sequencing. *Nat. Biotechnol.* **27**, 182–189 (2009).  
1039
- 1040 33. Carpenter, M. L. *et al.* Pulling out the 1%: whole-genome capture for the targeted  
1041 enrichment of ancient DNA sequencing libraries. *Am. J. Hum. Genet.* **93**, 852–64  
1042 (2013).  
1043
- 1044 34. Kalinowski, S. T., Taper, M. L. & Marshall, T. C. Revising how the computer  
1045 program CERVUS accommodates genotyping error increases success in  
1046 paternity assignment. *Mol. Ecol.* **16**, 1099–1106 (2007).  
1047
- 1048 35. Marshall, T. C., Slate, J., B., K. L. E. & Pemberton, J. M. Statistical confidence for  
1049 likelihood-based paternity inference in natural populations. *Mol. Ecol.* **7**, 639–655  
1050 (1998).  
1051
- 1052 36. Chakraborty, R., Shaw, M. & Schull, W. J. Exclusion of paternity: the current state  
1053 of the art. *Am. J. Hum. Genet.* **26**, 477–88 (1974).  
1054
- 1055 37. Alberts, S. C. & Altmann, J. in *Long-term F. Stud. primates* (Kappeler, P. M. &  
1056 Watts, D. P.) 261–287 (Springer, 2012).  
1057
- 1058 38. Alberts, S. C., Buchan, J. C. & Altmann, J. Sexual selection in wild baboons: from  
1059 mating opportunities to paternity success. *Anim. Behav.* **72**, 1177–1196 (2006).  
1060
- 1061 39. Morin, P. A., Chambers, K. E. K., Boesch, C. & Vigilant, L. Quantitative  
1062 polymerase chain reaction analysis of DNA from noninvasive samples for  
1063 accurate microsatellite genotyping of wild chimpanzees (*Pan troglodytes verus*).  
1064 *Mol. Ecol.* **10**, 1835–1844 (2001).  
1065
- 1066 40. Daley, T. & Smith, A. D. A. Predicting the molecular complexity of sequencing  
1067 libraries. *Nat. Methods* **10**, 325–329 (2013).  
1068
- 1069 41. Samuels, D. C. *et al.* Finding the lost treasures in exome sequencing data. *Trends*

- 1070            *Genet.* **29**, 593–9 (2013).  
1071
- 1072    42.    Lipatov, M., Sanjeev, K., Patro, R. & Veeramah, K. *Maximum Likelihood*  
1073            *Estimation of Biological Relatedness from Low Coverage Sequencing Data.*  
1074            *bioRxiv* (Cold Spring Harbor Labs Journals, 2015). doi:10.1101/023374  
1075
- 1076    43.    Sinnwell, J. P., Therneau, T. M. & Schaid, D. J. The kinship2 R package for  
1077            pedigree data. *Hum. Hered.* **78**, 91–3 (2014).  
1078
- 1079    44.    Thompson, E. A. & Meagher, T. R. Parental and sib likelihoods in genealogy  
1080            reconstruction. *Biometrics* **43**, 585–600 (1987).  
1081
- 1082    45.    Olsen, J. B., Busack, C., Britt, J. & Bentzen, P. The aunt and uncle effect: an  
1083            empirical evaluation of the confounding influence of full sibs of parents on  
1084            pedigree reconstruction. *J. Hered.* **92**, 243–7 (2001).  
1085
- 1086    46.    Ford, M. J. & Williamson, K. S. The aunt and uncle effect revisited - The effect of  
1087            biased parentage assignment on fitness estimation in a supplemented salmon  
1088            population. *J. Hered.* **101**, 33–41 (2010).  
1089
- 1090    47.    Ávila-Arcos, M. C. *et al.* Comparative Performance of Two Whole Genome  
1091            Capture Methodologies on Ancient DNA Illumina Libraries. *Methods Ecol. Evol.*  
1092            n/a–n/a (2015). doi:10.1111/2041-210X.12353  
1093
- 1094    48.    Enk, J. M. *et al.* Ancient whole genome enrichment using baits built from modern  
1095            DNA. *Mol. Biol. Evol.* **31**, 1292–4 (2014).  
1096
- 1097    49.    Van Horn, R. C., Altmann, J. & Alberts, S. C. Can't get there from here: inferring  
1098            kinship from pairwise genetic relatedness. *Anim. Behav.* **75**, 1173–1180 (2008).  
1099
- 1100    50.    George, R. D. *et al.* Trans genomic capture and sequencing of primate exomes  
1101            reveals new targets of positive selection. *Genome Res.* **21**, 1686–94 (2011).  
1102
- 1103    51.    Vallender, E. J. Expanding whole exome resequencing into non-human primates.  
1104            *Genome Biol.* **12**, R87 (2011).  
1105

- 1106 52. Palme, R. Measuring fecal steroids: guidelines for practical application. *Ann. N. Y.*  
1107 *Acad. Sci.* **1046**, 75–80 (2005).  
1108
- 1109 53. Ley, R. E., Lozupone, C. A., Hamady, M., Knight, R. & Gordon, J. I. Worlds within  
1110 worlds: evolution of the vertebrate gut microbiota. *Nat. Rev. Microbiol.* **6**, 776–788  
1111 (2008).  
1112
- 1113 54. Gillespie, T. R. Noninvasive Assessment of Gastrointestinal Parasite Infections in  
1114 Free-Ranging Primates. *Int. J. Primatol.* **27**, 1129–1143 (2006).  
1115
- 1116 55. Knight, J. M. *et al.* Non-invasive analysis of intestinal development in preterm and  
1117 term infants using RNA-Sequencing. *Sci. Rep.* **4**, 5453 (2014).  
1118
- 1119 56. Moll, P. R., Duschl, J. & Richter, K. Optimized RNA amplification using T7-RNA-  
1120 polymerase based in vitro transcription. *Anal. Biochem.* **334**, 164–74 (2004).  
1121
- 1122 57. Shagina, I. *et al.* Normalization of genomic DNA using duplex-specific nuclease.  
1123 *Biotechniques* **48**, 455–9 (2010).  
1124
- 1125 58. Roeder, A. & Archer, F. A novel method for collection and preservation of faeces  
1126 for genetic studies. *Mol. Ecol. ...* **4**, 761–764 (2004).  
1127
- 1128 59. Nsubuga, A. M. *et al.* Factors affecting the amount of genomic DNA extracted  
1129 from ape faeces and the identification of an improved sample storage method.  
1130 *Mol. Ecol.* **13**, 2089–94 (2004).  
1131
- 1132 60. Li, H. Aligning sequence reads, clone sequences and assembly contigs with  
1133 BWA-MEM. (2013).  
1134
- 1135 61. Landt, S. G. *et al.* ChIP-seq guidelines and practices of the ENCODE and  
1136 modENCODE consortia. *Genome Res.* **22**, 1813–31 (2012).  
1137
- 1138 62. Kharchenko, P. V, Tolstorukov, M. Y. & Park, P. J. Design and analysis of ChIP-  
1139 seq experiments for DNA-binding proteins. *Nat. Biotechnol.* **26**, 1351–9 (2008).  
1140

- 1141 63. R Development Core Team. R: A Language and Environment for Statistical  
1142 Computing. (2015).  
1143
- 1144 64. Li, H. *et al.* The Sequence Alignment/Map format and SAMtools. *Bioinformatics*  
1145 **25**, 2078–9 (2009).  
1146
- 1147 65. Li, H. A statistical framework for SNP calling, mutation discovery, association  
1148 mapping and population genetical parameter estimation from sequencing data.  
1149 *Bioinformatics* **27**, 2987–93 (2011).  
1150
- 1151 66. Van der Auwera, G. A. *et al.* From FastQ Data to High-Confidence Variant Calls:  
1152 The Genome Analysis Toolkit Best Practices Pipeline. *Curr. Protoc. Bioinforma.*  
1153 11.10.1–11.10.33 (2013). doi:10.1002/0471250953.bi1110s43  
1154
- 1155 67. McKenna, A. *et al.* The Genome Analysis Toolkit: a MapReduce framework for  
1156 analyzing next-generation DNA sequencing data. *Genome Res.* **20**, 1297–303  
1157 (2010).  
1158
- 1159 68. DePristo, M. A. *et al.* A framework for variation discovery and genotyping using  
1160 next-generation DNA sequencing data. *Nat. Genet.* **43**, 491–498 (2011).  
1161
- 1162 69. O’Rawe, J. *et al.* Low concordance of multiple variant-calling pipelines: practical  
1163 implications for exome and genome sequencing. *Genome Med.* **5**, 28 (2013).  
1164
- 1165 70. Tung, J., Zhou, X., Alberts, S. C., Stephens, M. & Gilad, Y. The genetic  
1166 architecture of gene expression levels in wild baboons. *Elife* **4**, e04729 (2015).  
1167
- 1168 71. Danecek, P. *et al.* The variant call format and VCFtools. *Bioinformatics* **27**, 2156–  
1169 8 (2011).  
1170
- 1171 72. Yang, J. *et al.* Common SNPs explain a large proportion of the heritability for  
1172 human height. *Nat. Genet.* **42**, 565–9 (2010).  
1173
- 1174 73. Manichaikul, A. *et al.* Robust relationship inference in genome-wide association  
1175 studies. *Bioinformatics* **26**, 2867–73 (2010).  
1176